Pathological Plasticity and Glutamate Transport in Fragile-X Tremor and Ataxia Syndrome

Honors Thesis in Neuroscience
University of Michigan

Arya Ahmady

TABLE OF CONTENTS

Abstract

Fragile-X Tremor and Ataxia Syndrome (FXTAS) is a progressive neurodegenerative disorder characterized by action tremor, gait difficulties, and dementia. It is caused by a 55-200 length CGG trinucleotide repeat expansion in the 5' untranslated region of the *FMR1* gene. If the repeat over 200 CGG's, FMRP is not produced, resulting in the most common inherited form of autism; Fragile X Syndrome. Research has shown deficits in network activity of Fragile X-related disorders, such as hyper excitability and epileptogenesis with relatively normal increases in neuronal activity. Defects in homeostatic plasticity, the way neurons regulate their own excitability relative to the network they are part of, or glutamate transport would account for the hyper excitability observed in FXTAS. In this study homeostatic plasticity and glutamate transport are examined in the CGG Knock-In mouse model then compared to wildtype and Fmr1 Knock-out cells. Overall, CGG KI cells show minimal change in GluR1 containing AMPA receptor expression following CNQX treatment, whereas wildtype and Fmr1KO cells show an increase following the same treatment. Furthermore while Fmr1KO cells demonstrated significantly lower Excitatory Amino Acid Transporter 2 levels, CGG KI cells demonstrated similar levels as those found in wildtype cells. To examine how these pathologies translate into observable behavior, motor coordination between the Dutch and NIH CGG KI mouse models was compared. These models differ in the way the CGG repeat is inserted upstream of the FMR1 gene, resulting in only the Dutch model having a polyglycine protein product. Only at the end stage, do the Dutch model and NIH CGG KI models mice exhibit subtle differences in motor coordination with each other, yet both significantly differed from wildtype mice. All in all these findings demonstrate key defects in neuronal plasticity that underlie the most pronounced pathologies observed in Fragile-X related disorders, thus illustrating potential targets for treatment.

Introduction

Fragile-X Syndrome (FXS) is currently the most common form of inherited intellectual disability. Symptoms include mild to severe cognitive delay, as well as behavioral characteristics such as stereotypic movements and social anxiety (Hagerman et al 2002). The condition is caused by a CGG trinucleotide repeat expansion in the 5' untranslated region (UTR) of the *FMR1* gene, which is located on the X chromosome (Oberle et al. 1991). This gene codes for the fragile X mental retardation protein, FMRP. When the CGG expansion is greater than 200 repeats, hypermethylation of the repeat sequence occurs as well as a neighboring CpG island within the *FMR1* promoter. This prevents the transcription of FMR1 mRNA, leading to the absence of FMRP and resulting in Fragile-X Syndrome (Verkerk et al 1991, Bardoni et al 2002, and Kaufmann et al 2002).

Mid-range premutation repeats (50-200 CGGs) cause a related allelic disorder, known as Fragile X-associated Tremor/Ataxia Syndrome (FXTAS). FXTAS is a progressive neurodegenerative disorder characterized by action tremor, gait difficulties, and dementia (Basuta et al 2011). The premutation range CGG repeat specific to FXTAS causes a stable secondary hairpin structure in the transcribed mRNA, which result in protein sequestration and toxic mRNA-mediated neurodegeneration culminating in FXTAS. In contrast with FXS, premutation CGG repeat expansions lead to increased expression of FMR1 mRNA, yet surprisingly research shows the expression of FMRP to be decreased in males affected with FXTAS (Tassone et al 2000; Renoux et al 2014; Pretto et al 2014; Ludwig et al 2014). Interestingly, the increased FMR1 mRNA

expression has been shown to be a result of increased FMR1 transcription, rather than increased FMR1 RNA stability (Tassone 2000; Todd et al 2010). In attempting to explain this finding, research has shown that the CGG repeat in FMR1 acts to impair translation by interfering with ribosomal scanning through the 5′UTR, subsequently preventing appropriate loading of CGG expanded FMR1 mRNA into polyribosomal complexes (Ludwig et al 2011, Darnell et al 2011). Through this mechanism, little FMRP can be translated despite increased amounts of the FMR1 mRNA.

FMRP is an RNA binding protein found associated with stalled ribosomes that regulates synthesis of proteins in response to synaptic stimulation (Ronesi and Huber et al 2008; Darnell et al 2011). When phosphorylated, FMRP can repress translation of a variety of mRNA transcripts (Laggerbauer et al. 2001). The FMRP protein itself has been shown to bind to hundreds of mRNA transcripts, suggesting that the phosphorylation of FMRP plays a crucial role in the regulation of protein production (Darnel et al. 2011). Interestingly, FMRP has been also shown to bind to and regulate the translation of its own mRNA *in vitro* as well as synaptic proteins such as PSD-95. (Jin et al 2000, Todd et al 2003).

The role of FMRP at the synapse is demonstrated by research showing increased FMRP translation in response to metabotropic glutamate stimulation (Todd et al. 2003, Hou et al 2006; Weiler et al 1997; Iliff et al 2013). At rest, FMRP is phosphorylated but upon mGluR activation, mGluR signaling induces dephosphorylation of FMRP, causing it to dissociate from polysome–transcript complexes (Narayanan et al 2007). It is then rapidly degraded, resulting in an activity-dependent burst of translation of the mRNAs that FMRP originally targeted (Nalavadi et al 2012).

As with many other diseases, it is crucial to establish an animal model that can duplicate the key pathologies of the disease at a molecular and behavioral level. Unfortunately no FXTAS mouse model exists that completely replicate all of the pathologies and symptoms reported in individuals affected with the Fragile-X Premutation or patients with FXTAS. Furthermore there have not been any reports of obvious tremor in current mouse models, which is a critical neurological feature of FXTAS (Berman et al 2014). The mouse models that are yet available only partially replicate pathologies of the Fragile-X Premutation (FPM) and FXTAS. (Bontekoe et al 2001).

To study the impact of the expanded CGG repeats in the 5'UTR of *FMR1*, two knock-in (KI) mouse models were generated (preCGG; Entezam et al 2007; Bontekoe et al 2001), in which a portion of the 5′ UTR from the human pre-mutation has been inserted into the mouse FMR1 gene (Tassone et al. 2000 and Singh et al. 2007). The first was a CGG KI mouse model from the Willemsen laboratory in the Netherlands, otherwise known as the Dutch mouse (CGGdut KI). This mouse model was created through replacing the native murine CGG repeat, which happened to be eight trinucleotides in length (CGG8), with a human CGG98 repeat. All of this was accomplished within the endogenous Fmr1 gene through the use of homologous recombination in embryonic stem cells. Fortunately this was done with minimal changes to the murine Fmr1 promoter while including the region flanking the repeat in the human *FMR1* gene. Interestingly the Dutch model mice are able to show moderate instability of repeat length upon paternal and maternal transmission. (Berman et al 2014; Bontekoe et

al 2001). Additionally this model is also able to replicate the pathology seen in affected Fragile-X Premutation (FPM) carriers and in FXTAS, including increased expression of Fmr1 mRNA, decreased FMRP, ubiquitin-positive intra-nuclear inclusions, and evidence for motor and spatial processing deficits (Berman et al 2014).

A second knock-in mouse was developed at the National Institutes of Health with an initial 118 CGG repeat tract (Entezam et al 2007). This was accomplished through the use of a targeting construct that retrofitted two adjacent but incompatible *Sfi* I sites in the exon 1 of the mouse Fmr1 gene. The *Sfi* I sites are places, in which a specific restriction enzyme may cut the DNA. As a result, the repeats were flanked by the appropriate *Sfi* I sites, allowing the CGG repeats to be inserted into the mouse locus in the correct orientation while minimally changing the mouse flanking sequence. Subsequently the NIH mouse model retains the translational TAA stop codon just upstream of the CGG118 repeat, which is only in endogenous murine gene. Similar to the Dutch mice, the NIH mice show elevated *Fmr1* mRNA levels, decreased FMRP levels, moderate intergenerational expansions, no methylation and ubiquitin-positive intranuclear inclusions (Entezam et al 2007).

Both the Dutch and NIH CGG Knock in mouse models show several-fold increases in levels of Fmr1 mRNA, a reduction in brain levels of FMRP, and decreased FMRP expression with larger pre-mutation repeat lengths (Entezam 2007, Illif et al 2013, Qin et al 2011). However, the Dutch mouse model shows a (20% to 30%) reduction in FMRP, while the NIH model shows a >50% reduction (Todd et al 2013). Behaviorally, both models show progressive deficits in processing spatial information, cognitive deficits, motor deficits, and hyperactivity. Nonetheless, the Dutch model mouse shows

increased anxiety, while the NIH model shows decreased anxiety (Qin et al 2011). Most notably, NIH KI mouse retains more of the mouse 5′UTR flanking the CGG repeat, which includes the TAA stop codon that is not present in the Dutch model. It has been suggested that the absence of this stop codon in the CGGdut KI may allow RAN translation of a novel polyglycine protein that contributes to CGG repeat toxicity in human cell lines (Todd et al 2013).

Hippocampal neurons cultured from the Dutch model CGG-Knock In mice show impairments in dendritic complexity and an altered architecture of synapsin puncta prior to neurodegeneration (Chen et al 2009). Studies using other models have shown a combination of deficits in network activity in Fragile X-related disorders resulting in increased susceptibility to hyper excitability and epileptogenesis when faced with relatively normal increases in neuronal activity (Musumeci et al. 2007). Furthermore CGG-KI mice show increased mRNA levels of many components of the GABAergic system in the cerebellum but not in the cortex, suggesting altered inhibitory neuronal transmission in the CGG-KI mice (D'hulst et al 2009). All together these findings demonstrate a state of hyperexcitablity in the CGG-KI mouse model.

To understand how pathological excitability is caused in cells, it is essential to understand key synaptic receptors. One of the most prominent types of receptors in neurons are ionotropic AMPA receptors (AMPARs), which are named after an agonist that mimics the effect of glutamate binding (Amino-3-hydroxy-5-methyl-4-isoxazolepropionic acid). The more AMPARs a cell has, the more current is likely to pass through during every presynaptic vesicle release. AMPARs are composed of four subunits, GluR1, GluR2, GluR3, and GluR4. Interestingly, if the GluR2 subunit is absent,

then the AMPAR will be permeable to sodium, potassium, and calcium. If the GluR2 subunit is present, the AMPAR channel will almost always be impermeable to calcium (Kim et al 2001). On the contrary NMDA receptors, named after the agonist N-methyl-D-aspartate, are ionotropic glutamate channels that are voltage and ligand-gated. Thus at a particular voltage, the extracellular magnesium block will leave the channel and allow sodium and potassium ions to pass through (Laube et al 1997). The passage of Calcium through NMDARs is thought to be a critical component of synaptic plasticity as well as a cellular mechanism for learning and memory (Kleckner et al 1988).

Research has shown pathological plasticity in excitatory hippocampal synapses of the *Fmr1* KO mice through exaggerated protein translation and Group 1 metabotropic glutamate receptor (mGluR)-dependent depression (Huber et al 2000). The "mGluR theory of FXS" claims that FMRP is a downstream regulator of Group 1 mGluR activation (Bear et al 2004). FMRP has shown to be upregulated in the presence of the Group 1 mGluR agonist Dihydroxyphenylglycine (DHPG), which induces Long Term Depression (LTD) in the CA1 region of the hippocampus (Illif et al 2012). In this form of LTD, ionotropic glutamate receptors, undergo internalization, thus decreasing synaptic strength in response to DHPG (Huber et al 2000). In the complete absence of FMRP, mGluR-LTD is enhanced but no longer requires new protein synthesis (Nosyreva et al 2006). Therefore newly synthesized FMRP negatively regulates further local translation, thus constraining the magnitude of LTD after mGluR activation (Bear et al 2004).

To understand the full nature of pathological plasticity in FXTAS, one must also examine the role of FMRP in regulating synaptic function. Homeostatic Plasticity (HSP) refers to the ability of neurons to regulate their own excitability relative to the network

that they are a part of. Neurons have a preferred firing pattern, and if there is any deviation from this pattern, neurons can compensate to return to that set point (Marder & Prinz, 2002). Networks that operate purely by Hebbian plasticity rules have been shown to be inherently unstable due to the positive feedback nature of Long Term Potentiation (LTP) and Long Term Depression (LTD) because there is no way to control for excessive coincidental presynaptic input (Miller et al. 1996). The earliest studies of HSP were performed in the crustacean stomatogastric ganglion. It was found that when rhythmically firing neurons were isolated, their rhythmic activity was abolished. However after the neurons were returned to culture, rhythmic firing had in fact returned. (Turrigiano et al. 1994).

There are two types homeostatic plasticity: global HSP and local HSP. Global HSP is observed after chronic blockade (48 hours) of action potentials in cultured neurons with the voltage-gated sodium channel antagonist tetrodotoxin (TTX). Blocking neurons with TTX produces a compensatory increase in miniature Excitatory Post Synaptic Potential (mEPSP) amplitudes due to a transcription-dependent accumulation of GluA2-containing AMPARs (Gainey et al. 2009). On the contrary, Local HSP is observed by blocking NMDA receptors and action potentials (TTX+APV) in cultured hippocampal neurons. In turn, this leads to an increase in the amplitude of mEPSCs within 60 minutes (Sutton et al. 2006). AMPAR blockade in place of NMDAR blockade can lead to similar results, however this treatment has demonstrated presynaptic changes (Henry et al., 2012; Jakawich et al., 2010).

Synaptic scaling is a well-studied form of HSP that is induced by long-term blockade of neuronal firing and synaptic transmission, such as in local and global HSP.

However this process can be detected through evidence of new synthesis and insertion of the ionotropic AMPAR. (Thiagarajan et al., 2005; Sutton et al., 2006; Aoto et al., 2008). One molecule involved in synaptic scaling is Retinoic acid (RA), which binds to the retinoic acid receptor RARα. This receptor normally inhibits protein translation by binding with specific target mRNA's and inhibiting translation (Poon and Chen 2008). Addition of RA relieves the translation block RARα has on its target mRNA. Interestingly the mRNAs for GluR1 and GluR2 are some of the targets of RARα (Muddashetty 2007).

FMRP has been shown to play an important role in the mechanism of HSP (Soden and Chen et al 2010). Research has demonstrated that CA1 pyramidal neurons show increased mEPSC amplitude following TTX+APV treatment. However they did not see this finding in CA1 neurons from Fmr1 KO mice (Soden and Chen et al 2010). They used a retinoic acid response element that controlled GFP transcription to show RA activity. Using this technique they demonstrated that introduction of a viral vector of FMRP to Fmr1 KO cell cultures can restore RA-induced signaling in CA1 neurons. Surprisingly, although activity-dependent RA synthesis is maintained in Fmr1 knockout neurons, RA-dependent dendritic translation of GluR1-type AMPA receptors is impaired. Postsynaptic expression of wild-type or mutant FMRP (I304N prevents the binding of FMRP to target mRNA's) in knockout neurons reduced the total, surface, and synaptic levels of AMPA receptors, hence suggesting a role for FMRP-regulated protein translation in controlling synaptic AMPAR abundance. In conclusion they argue that FMRP is essential for increases in synaptic strength induced by RA or by blockade of neuronal activity, but that the action of FMRP occurs downstream of RA.

Remarkably little research has been performed to understand how the fragile-X premutation might impact HSP. It has been demonstrated earlier that mGluR-LTD is altered in the permutation mice, but it is not clear whether the impaired activity dependent FMRP resulting from the expanded CGG repeat will also impact HSP. Perhaps HSP will be altered in a pathological way, similar to the FMR1 KO phenotypes or possibly retain properties of the wildtype phenotype.

Another potential mechanism that may underlie hyperexcitability in FXTAS may be alterations in the Glutamate-Glutamine cycle. The action of this cycle is critical to maintaining the neurotransmitter glutamate in the synapse in addition to recycling excess glutamate (Westergaard et al 1995). Impaired glutamate transport contributes to the neurotoxicity of many pathological processes, including stroke/ischemia, temporal lobe epilepsy, Alzheimer's disease, amyotrophic lateral sclerosis, Huntington's disease, HIV-1-associated dementia, and growth of malignant gliomas (Su et al 2002). A defect in this cycle could contribute to the neuronal dysfunction observed in FXTAS. Glutamate transporter 1 (GLT1) is the murine homologue of the human excitatory amino acid transporters (EAAT 1-3), which is an astrocytic glutamate transporter. Glutamate transporters are primarily localized in glial cells although their expression has also been detected in neurons (Zhou et al 2005). EAAT1 and EAAT2 are the principal means by which glutamate is recycled in the central nervous system and it is estimated that EAAT2 clears over 90% of Glu alone (Danbolt et al 2001). However EAAT1 is the main transporter in the cerebellum (Rose et al 2009).

After glutamate has been released from the presynaptic cell, either the presynaptic neuron reuptakes the glutamate or passes glutamate through the EAAT1 or EAAT2 on

astrocytes. Within the astrocyte, glutamate is converted to glutamine through the enzyme Glutamine Synthetase. Glutamine is then transported out of astrocytes and is taken up by the presynaptic neuron, where it is converted back into glutamate through the enzyme Glutaminase. Additionally the presynaptic nerve terminal also has EAAT3 transporters than can directly transport excess glutamate back into the presynaptic neuron (Danbolt et al 2001).

Interestingly upregulation of GLT1 severely impairs one form of synaptic plasticity, long-term depression (LTD), at mossy fibre-CA3 synapses (Omrani et al 2009). One recent report found that astroglial GLT1 and glutamate uptake is significantly reduced in the cortex of Fmr1 KO mice (Higashimori et al 2013). Furthermore, this study demonstrated that FMRP-deficient astrocytes derived from fmrp KO mice are capable of inducing abnormal dendritic morphology of wild-type hippocampal neurons in vitro. Fmr1 KO astrocyte and WT neuron co-cultures turned out to have the lowest GLT1 protein levels (Higashimori et al 2013). In contrast, GLT1 protein levels in WT astrocyte and Fmr1 KO neuron co-cultures were only slightly reduced compared with those of WT co-cultures (Higashimori et al 2013). With more glutamate in the synapse, neurons of Fmr1 KO cells would be subsequently more prone to hyperexcitablility.

An even more recent report showed reduced excitatory amino acid transporter 1 (EAAT1) levels and mGluR5 expression in the cerebellum of post-mortem human permutation carriers with FXTAS (Pretto et al 2015). It has been further demonstrated that there are decreased levels of VGLUT and VGAT in mice PreCGG hippocampal neurons, along with astrocytes having decreased glutamate uptake (Cao et al 2012). VGLUT and VGAT are vesicular transporters that are responsible for the loading of

glutamate and GABA into presynaptic vesicles. Perhaps these defects in glutamate transport might be acting in conjunction with alterations in HSP to exacerbate the pathology observed in FXTAS.

I hypothesize that neuronal susceptibility to hyper excitability observed in FXTAS can be attributed to defects in homeostatic plasticity and glutamate recycling. To investigate this hypothesis I propose several aims in which to examine.

First I plan to determine changes in homeostatic plasticity seen in between CGG KI and wildtype-cultured neurons. I believe that basal surface AMPA receptor expression will be increased in CGG KI compared to wild type cultured neurons. Furthermore, when all AMPA receptors are blocked using only the AMPA receptor antagonist CNQX, the CGG KI neurons will not show an increase in surface AMPA receptors as expected in wildtype cells. This would explain the increased hyperexcitability of these neurons. To test this, I plan to see how surface AMPA receptor levels change in the presence of a CNQX, in wildtype and FXTAS mouse model neurons. Specifically I will use immunocytochemistry to measure surface levels of the AMPA receptor subunit GluR1 to examine this hypothesis. In addition I will subsequently repeat these experiments in the Fmr1 KO mouse, a mouse model of Fragile-X Syndrome, to see if the CGG repeat expansion yields different results.

Secondly, I aim to determine levels of GLT1 in wildtype and CGG KI glia. I expect to see a lowering of GLT1 in CGG KI astrocytes, but I predict that GLT1 levels will still remain higher than those found in Fmr1 KO glia which lack FMRP expression.

I will test this aim by first quantifying the basal levels of GLT1 in GFP-labeled wildtype and Fmr1 KO hippocampal co-cultures. Then I will repeat the same procedure in the wildtype and CGG KI mice cell co-cultures. GLT1 will be measured in glia marked with the glial fibrillary acidic protein (GFAP) to distinguish them from neurons in the same culture.

Lastly I aim to take a different approach to determine the effects of the CGG KI genotype on motor behavior. Specifically I will examine both the Dutch and NIH mouse model to determine any differences in motor coordination. This in turn will further validate both of these mouse models as a proper model to study FXTAS, while simultaneously determining which one shows the greatest discrepancy with the wildtype model. Although I believe that both CGG-KI mouse models should display significant defects in motor coordination compared to wildtype mice, I hypothesize that the NIH model will show greater discrepancies to the wildtype mice because they show a greater reduction in FMRP compared to the Dutch model (Todd et al 2013). To test this, I will subject wildtype and CGG KI mice from both models to a motor test that involves crossing a balance beam. I will compare crossing time, number of falls, and foot slips, as a means to experimentally measure coordination. Mice will be observed at 12, 18, and 24 months of age to monitor age-dependent decrements in this motor task.

Materials and Methods

Western Blotting

Protein lysates were obtained from the cortex and cerebellum of wildtype and CGG KI mice, both of which were rapidly prepared from flash frozen tissue samples. Tissue samples were lysed in a RIPA buffer solution containing protease inhibitors (1 pill/10mL of solution) to prevent degradation. Samples were then sonicated to dissociate larger organelles and cleave genomic DNA for better separation with SDS-PAGE. The samples were then spun down at 13,000 rpm for 8 min in a centrifuge, after which the supernatant was collected while the pellet discarded. Some insoluble RAN translation products are in the pellet, however they were not needed for the purpose of this experiment. The final protein concentration was obtained manually using a DC protein assay. A sample of BSA was diluted into RIPA buffer at varying concentrations to generate a standard curve for the protein assay, while brain lysate samples were diluted at 1:5 and 1:10, and tested in triplicate for final measurements. Dilutions and standard curve samples were mixed with colorimetric reagents and the optical absorbance at 750nm of light was used to measure protein content.

A total of 50 μg of protein and 10 μL of 6x LSB were prepared each lane, while any differences were made up by adding more or less RIPA buffer to end up with 60 μL of solution per lane. Freshly made lysates were held at 95°C for 5 min, then left to cool. Samples were then loaded and run at 190mV on an 8% acrylamide gel and transferred onto a membrane overnight at 32mV. Afterwards the blots were probed with a rabbit α-FMRP antibody at 1:5000 and a mouse α-tubulin antibody at 1:5000 both of which were

prepared in a 5% NFDM blocking solution. Following a similar procedure, the secondary fluorescent antibodies were prepared as 1:15,000 with 1:100 of 10% SDS in a 5% NFDM solution. The secondary antibody for FMRP was goat anti-rabbit Alexa Fluor 433 while that of tubulin was goat anti-mouse Alexa Fluor 533. The membranes were washed in TBS-T and visualized with the LI-COR Odyssey. The specific colors on the image were arbitrarily chosen by the Odyssey to distinguish different proteins and do not reflect the actual colors of the bands on the membrane. The green color represents FMRP bands, while the red represents tubulin bands.

The brain lysates of four different mice from the CG 149 cage, which housed two wildtype and two NIH CGG KI mice, were used in the experiment. To verify that the samples are in the linear range and not saturated, every sample is given two lanes: one with a 1x concentration while the other is given a 2x concentration. If the loading was accurate, the 2x lane of each sample should fluoresce at twice the intensity of the 1x lane, otherwise the data is excluded. Thus the brain lysate from each animal was loaded into two lanes on the gel. Only the 1x samples were analyzed, and subsequently only the FMRP bands at 75kD are used for analysis. The fluorescence of the FMRP bands in each lane is normalized to the tubulin band of the same lane, thus FMRP is normalized to tubulin. The average ratio of all of the wildtype samples is obtained, and then the FMRP to Tubulin ratio of each lane (wildtype and CGG KI) is divided by the average wildtype ratio. This allows one to see any change in experimental and control values relative to a standard control value.

Surface GluR1 Staining

The cells were 14-17 day old GFP/KO or GFP/CGGKI female mouse primary hippocampal neurons, thus allowing visualization of wildtype, Fmr1 KO, or CGG KI cells in the same culture. If the cell expresses GFP, it is expressing the wildtype X chromosome and if no GFP is expressed, then the cell has the CGGKI or Fmr1 KO mutation on its X Chromosome. Half of the cells were treated with CNQX for 6 hours, while the other half were treated with filtered neural growth media (NGM) as a control. A rabbit anit-GluR1 antibody was used at a concentration of 1:100 diluted in live media to label the cells live. After one hour and three washes in PBS-MC the cells were fixed with for 20 min in 2% paraformaldehyde then washed three times in PBS-MC. Next they are blocked in 2% BSA for 20 minutes, then labeled with 1:500 Alexa fluor anti-rabbit 555 secondary antibody diluted in 2% BSA. After another wash, the cells were permeabilized with 0.1% Triton-X in PBS-MC for 5 min, then blocked again for 20 min in BSA. Mouse α-PSD-95 (1:200) diluted in 2% BSA is added overnight. Cells are then washed 3 times, for 5 min per wash in PBS-MC, then 1:500 Alexa fluor anti-mouse 635 secondary antibody diluted in 2% BSA is added for 1 hour. Lastly the cells are again washed 3 times with 5 min per wash in PBS-MC. After washing, the cells were image on a confocal microscope.

To quantify the data, each dendrite was straightened using ImageJ, and analysis was restricted to dendrites. GluR1 expression was only quantified at puncta that expressed PSD-95. The threshold for how much fluorescence qualifies as a puncta is arbitrarily determined and is kept constant for all dendrites analyzed during the experiment. Masks of the images in the PSD-95 channel were then made onto the GluR1

channel, so that GluR1 fluorescence was restricted to PSD-95 puncta, which is the region of interest in this case. The raw values of each experimental group (wildtype control, wildtype CNQX, KO/KI control, KO/KI CNQX) were all normalized to the average wildtype control value.

Glutamate Transporter Staining:

The cells were 25 day old GFP/KO or GFP/CGGKI female mouse primary hippocampal neurons from the same culture as those used in the surface GluR1 staining. Thus glia that expressed GFP were wildtype and those that did not were either CGGKI or Fmr1KO. Cells were taken out of the incubator and fixed with 2% PFA for 20 minutes, then washed 3 times for 1 minute per wash in PBS-MC. Cells are then permeablized with 0.1% Triton-X for 5 minutes then blocked with 2% BSA for one hour. Then the primary rabbit EAAT2 antibody is applied at 1:1000 simultaneously with the mouse GFAP primary antibody at 1:1500, all diluted in 2% BSA with 100 microliters per plate. Cells are stained in primary overnight then washed 3 times for 5 min per wash with PBS-MC. The secondary antibody is applied with 1:1500 of the anti-rabbit Alexa Fluor 555 and 1:2000 of the anti-mouse Alexa Fluor 635 all diluted in 2% BSA with 100 microliters per plate. After one hour of staining, the cells are washed 3 times for 5 min per wash with PBS-MC then imaged on the confocal microscope.

For analysis, EAAT2 expression was localized to GFAP expression in the glia and all computations were done using ImageJ. The areas of the glia were traced from the images, using GFAP expression as a marker for tracing and distinguishing glia from neurons. Within each selected area, EAAT2 and GFAP expression are quantified, thus

restricting quantification to the cell. This would ensure that only fluorescence from glia are analyzed without background fluorescence from neurons. After image processing, EAAT2 expression of each genotype is divided by the average wildtype EAAT2 expression obtained in the cell area. Only in the wildtype and CGG KI cells are ratios of EAAT2 to GFAP analyzed, while only EAAT2 expression is analyzed in the GFP/Fmr1 KO culture (See pg. 23). Subsequently the raw fluorescence values of these two genotypes are normalized to the average wildtype EAAT2 to GFAP ratio.

Motor Behavior Test:

Both wildtype and CGG KI mice were analyzed on how they were able to cross a balance beam spanning the width of two platforms. The starting platform was clear on the starting side, which made the mice feel uncomfortable. Because the platform on the other side was opaque, this motivated the mice to cross the balance beam to get to this side. A round balance beam was used in addition to a more difficult square beam to gauge adaptation.

Image 1. Balance beam apparatus. Mice start on the clear platform (right) and cross to the box (left)

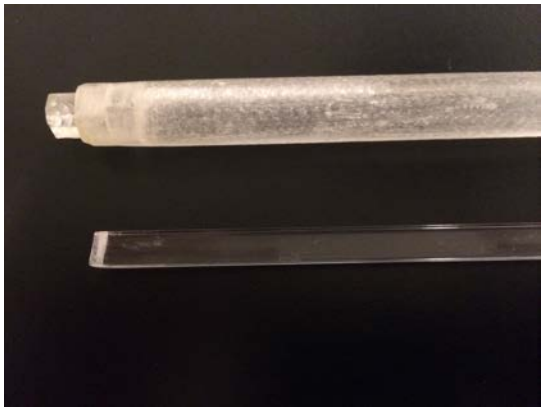

Image 2. Balance Beams. The round beam (top) and the more difficult square beam (bottom)

Testing consisted of four days with each mouse undergoing four trials across the beam. On the first day, a mouse would undergo a practice run which was not scored followed by two runs on the round beam and two runs on the square beam, both of which were scored. Days 2-4 consisted of only two runs on the round beam and two runs on the square beam, all of which were scored.

Scoring consisted of measuring how fast the mice crossed the beam, how many times their feet would slip while crossing (referred to as foot slips), how often they would pause, whether they dragged their hind legs while crossing instead of using all four legs, and if they fell. For quantification purposes, a fall was recorded as 30 seconds, a time where even the slowest mouse did not come close to. To observe any changes in motor behavior over time, mice were examined at 12, 18, and 24 months.

The results of all experiments, including western blotting, Immunocytochemistry, and behavioral, were analyzed by normalizing each of the raw values over the average control value. This in turn would determine the percent increase or decrease of the experimental group directly over the control. Statistical tests were performed using one tailed independent t-tests for the control and experimental groups of the ICC experiments, while two tailed t-tests were for each comparison in the behavioral studies.

Results

CGG Knock in Mouse model exhibited decreased FMRP expression compared to wild type control.

In this experiment, western blotting from two of the NIH model CGG Knock-In mice was used to demonstrate differences in FMRP expression in the cortex (Figure 1). Mice were from the CG 149 cage and were sacrificed at 24 months old. Previous literature has demonstrated decreased FMRP expression in CGG KI mice and in FXTAS patients (Entezam et al 2007, Tassone et al 2000, Pretto et al 2014; Ludwig et al 2014). The sample size in this experiment was small (N=2 wildtype; N=2 CGG KI), thus making it difficult to perform any statistical tests. Although there were several FMRP bands on the blot (200kD, 75kD, 60kD, and 50kD), only the FMRP values at 75kD were analyzed, since this is the reported size of FMRP described in the literature (Feng et al 1997, Laggerbauer et al 2001, Jin et al 2000). The smaller sized bands were most likely fragments of FMRP degraded through sample preparation, while the larger size bands were likely FMRP molecules that aggregated together and were not able to move through the gel appropriately. Lastly both the FMRP and tubulin bands in KI 2 of Figure 1a appear dimmer than the other samples. This could have been the result of improper loading or decreased protein concentration in the sample. Several repeats of this experiment are needed to successfully conclude decreased FMRP levels from this specific experiment.

Increased surface GluR1 expression at PSD-95 puncta of wildtype mouse neurons following CNQX treatment.

Prior to surface GluR1 staining, neuronal cultures treated with CNQX or NGM media (control) were imaged separately. GluR1 fluorescence intensity analysis was isolated only to PSD-95-positive puncta in the dendrites of each neuron (See pg. 16 for further description). This way even though several images displayed different fluorescence intensities, the intensities could be normalized for every cell. Only surface GluR1 expression is examined at PSD-95 puncta and is not normalized to PSD-95 expression. Previous literature has demonstrated that PSD-95 mRNA is unstable in the absence of FMRP, resulting in lower PSD-95 protein levels (Zalfa et al 2007), thus normalizing to PSD-95 expression would not be a valid control. The amount of GFP expressed per cell was not quantified, because it was not used in analysis. It only served as a marker to show which cells were wildtype or mutant. After image processing, the following results were obtained: Wildtype control: N=25, wildtype CNQX: N=24. Following CNQX treatment, wildtype neurons showed a statistically significant 61% increase in surface GluR1 expressed receptors (1.00±0.10 vs 1.61±0.25; p=0.01 Figure 2c). This finding agrees with previous results demonstrating that synaptic scaling does in fact require AMPA receptor regulation (Gainey et al 2009). Thus treatment with CNQX for six hours can induce increased surface GluR1 expression in wildtype neurons.

Slightly increased basal surface GluR1 expression at PSD-95 puncta of CGG-KI mouse neurons, but no significant difference following CNQX treatment.

Within each culture, wildtype GFP expressing neurons were analyzed separately from CGG KI neurons not expressing GFP. CGG KI control: N=23, CGG KI CNQX: N=28. Again all data was normalized to the wildtype control average. Contrary to wildtype cells, CNQX treatment in CGG KI cells did not yield a significant change in surface GluR1 fluorescence when compared to treatment with media (1.00±0.11 vs 0.94±0.07; p=0.35: Figure 3c). In examining basal surface GluR1 expression, although CGG KI cells in the same culture demonstrated increased surface GluR1 expression, the difference was not statistically significant (1.28±0.16 vs 1.00±0.10; p=0.06: Figure 4a). Following CNQX treatment, wildtype cells demonstrated a 61% increase in GluR1 expression while CGG KI cells showed a 6% decrease in surface GluR1 expression, essentially a minimal change (Figure 4b). Thus CNQX treatment fails to induce in externalization of GluR1 receptors at 6 hours in CGG KI mice, while there is enhanced externalization in WT mice.

Decrease basal GluR1 expression at PSD-95 puncta of Fmr1 Knock Out mouse neurons, but showed significant increase after CNQX treatment.

Neurons were separated and analyzed in the same method as mentioned as above, however cells that did not express GFP had the Fmr1 gene knocked out. After image processing, the distribution of cells were as follows: Wildtype control: N=26, Wildtype CNQX: N=31, Fmr1 KO control: N=24, and Fmr1 CNQX: N=12. Contrary to the results of the CGG KI cells, GluR1 fluorescence was significantly lower in the control Fmr1 KO

neurons as opposed to the wildtypes by about 15% (wildtype control: 1.00±0.04, Fmr1KO control: 0.85±0.05; p=0.013, Figure 6a). Fmr1 KO cells behaved similarly as the wildtype cells in Figure 2c, showing a significant 43% increase in surface GluR1 fluorescence following CNQX treatment (Fmr1KO control: 1.00±0.06, Fmr1 KO CNQX: 1.44±0.10; p=0.0001: Figure 5c). When compared to the CNQX mediated increase of surface GluR1 expression in wildtype cells, the Fmr1 KO cells exhibited a similar response (Figure 6b). This suggests that Fmr1 KO cells can demonstrate HSP more so than CGG KI cells.

Fmr1 KO mice exhibit significantly less Excitatory Amino Acid Transporter 2 levels relative to wildtype mice.

These cultures were derived using the XGFP culture system used in surface GluR1 staining, where GFP expression indicates the wildtype genotype while no GFP expression indicates the Fmr1KO genotype (XGFP/Fmr1 KO). Following image processing, the distribution of cells were Wildtype: N=23 and Fmr1KO: N=16. EAAT2 and GFAP fluorescence intensity was measured for individual glia. Previous research has indicated that GFAP expression is significantly up-regulated in the striatum, hippocampus, and cerebral cortex of Fmr1 knockout mice compared to wild-type mice (Yuskaitis et al 2010). Thus in the GFP/Fmr1KO cell culture, GFAP would not serve as a proper control to normalize to. Therefore only EAAT2 expression was quantified in this cell culture, only in the area where GFAP was expressed. When EAAT2 levels of both

genotypes were normalized to the average wildtype control levels, EAAT2 levels were significantly lower in Fmr1 KO cultures as compared to wildtype (wildtype: 1.00±0.08, Fmr1KO: 0.77±0.10, p=0.04, Figure 7c). This finding is consistent with previous results showing decreased GLT1 and EAAT1 levels in Fmr1 KO cell culture (Higashimori et al. 2013).

CGG KI mice exhibit no statistically significant decrease in Excitatory Amino Acid Transporter 2 levels.

The glia used in this experiment were derived using the XGFP culture system as mentioned above, however no GFP expression indicates the CGG KI genotype (XGFP/CGG-KI). Images were analyzed using the same procedure as above, studying EAAT2 and GFAP expression in the area of the cell. The distribution of cells analyzed were as follows: wildtype: N=27, CGG KI: N=17. Upon comparing Figure 8a to Figure 7a, it appears that the wildtype control EAAT2 levels were higher in the GFP/Fmr1KO cultures than the GFP/CGG KI cultures. The confocal microscope underwent repair in between the time the Fmr1KO and CGG KI samples were collected. Furthermore this was not due to a difference in EAAT2 expression because in both experiments EAAT2 fluorescence in the GFP/CGG KI cultures seemed dimmer in both genotypes. More likely this could have been a difference in uptake of the antibody. Since EAAT2 fluorescence in each was normalized to GFAP, any difference between each cell could be accounted for. There was no significant difference in raw GFAP levels between wildtype and CGG KI cells (p=0.2), thus validating GFAP expression as a reliable control to normalize to in this

experiment only. CGG KI glia showed similar EAAT2 to GFAP ratios as wildtype glia, (wildtype: 1.00±0.05, CGG KI: 0.87±0.07, p=0.06, Figure 8c). Furthermore, raw EAAT2 levels were compared between the two and again there was no significant difference between the wildtype and CGG KI glia (wildtype: 1.00±0.05, CGG KI: 0.97±0.07, p=0.36). Thus CGG KI glia showed normal EAAT2 expression.

Dutch and NIH CGG Knock-In mice demonstrate significant end-stage defects in motor coordination over the course of two years, compared to wildtype mice.

Upon reaching 12 months of age, mice were tested on a round beam and a more difficult to traverse square beam. At the time of testing, the wildtype, NIH, and Dutch model mice exhibited little differences in average time to cross either beam (Figure 9a). Although the average number of foot slips was higher in the Dutch mice on the first day for the round beam, the difference was not significant when compared to wildtype and NIH mice (Figure 11a). Furthermore during the 18-month testing period, the Dutch and NIH mice again showed little difference in crossing times during each of the days. The difference in the number of foot slips did not prove to be significant with either genotype as well (Figure 11b), suggesting that any aberration in motor coordination of either CGG KI mice was not present. On the testing after 24 months, the wildtype mice consistently crossed either beam significantly faster than both of the CGG KI mouse models on every day of testing (Figure 9c). During Day 1 on the round beam, the Dutch and the NIH mice crossing times differed little from each other, however on the square beam the NIH

differed from wildtype more so than the Dutch. Over time, the difference in crossing times between the Dutch and NIH model subsided, yet they were still both significantly longer than the wildtype. Additionally the wildtype mice were also able to cross both beams with greater coordination, as determined by the number of foot-slips (Figure 11c). The wildtype mice at the 24-month time point had fewer foot slips than both models, while no difference existed between the models.

Specific NIH CGG KI and Wildtype mice demonstrate end stage differences in motor coordination.

Only data from the mice in a particular cage were ready to be analyzed over the course of testing, thus yielding data from four mice (Wt N=2, NIH N=2). Both genotypes of mice exhibited similar crossing times for either beam during the 12-month and 18-month periods, however the wildtype mice seemed to exhibit faster crossing times during the 24-month period (Figure 12a). As expected with age, wildtype and NIH model mice appeared to exhibit an increase in crossing time with age. However this increase was more pronounced in the NIH model mice (Figure 12a and 12b). Although the NIH model mice appeared to demonstrate more foot slips, there seemed to be no difference in the number of foot slips between either genotype (Figure 12b).

Figures

a)

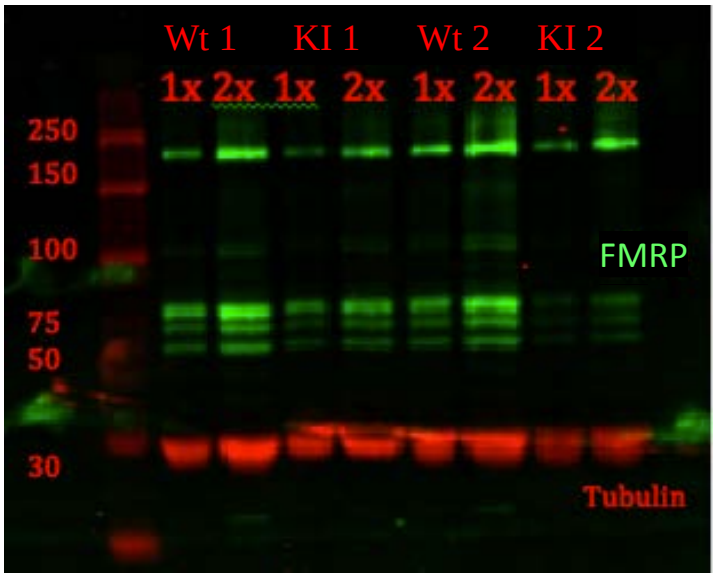

b)

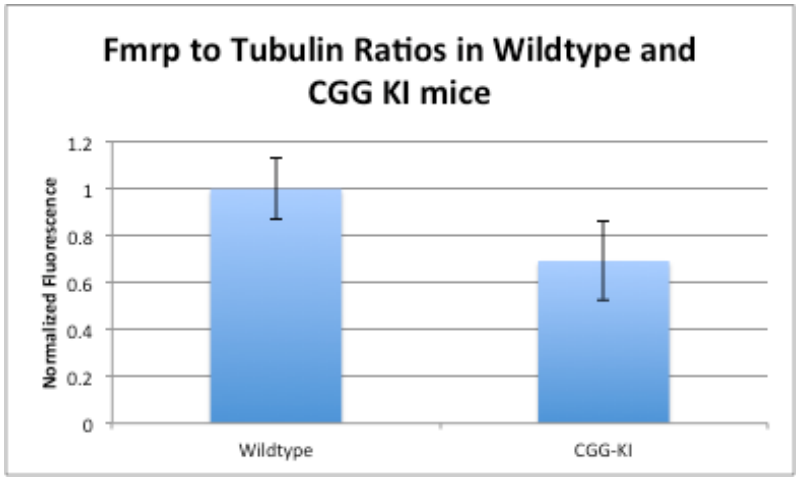

Figure 1. FMRP Expression in the CGG Knock-in Mouse model.

(a) Western blot of cortex lysate in two control and two NIH CGG KI mice. Each sample was loaded at 1x and 2x concentrations to demonstrate linearity. Only the FMRP bands at 75kD were analyzed. (b) Quantified results of the FMRP to tubulin ratios. The 75kD FMRP bands of each lane were normalized to their subsequent tubulin bands. All data was normalized to the average wildtype ratio.

a) Control

b) CNOX

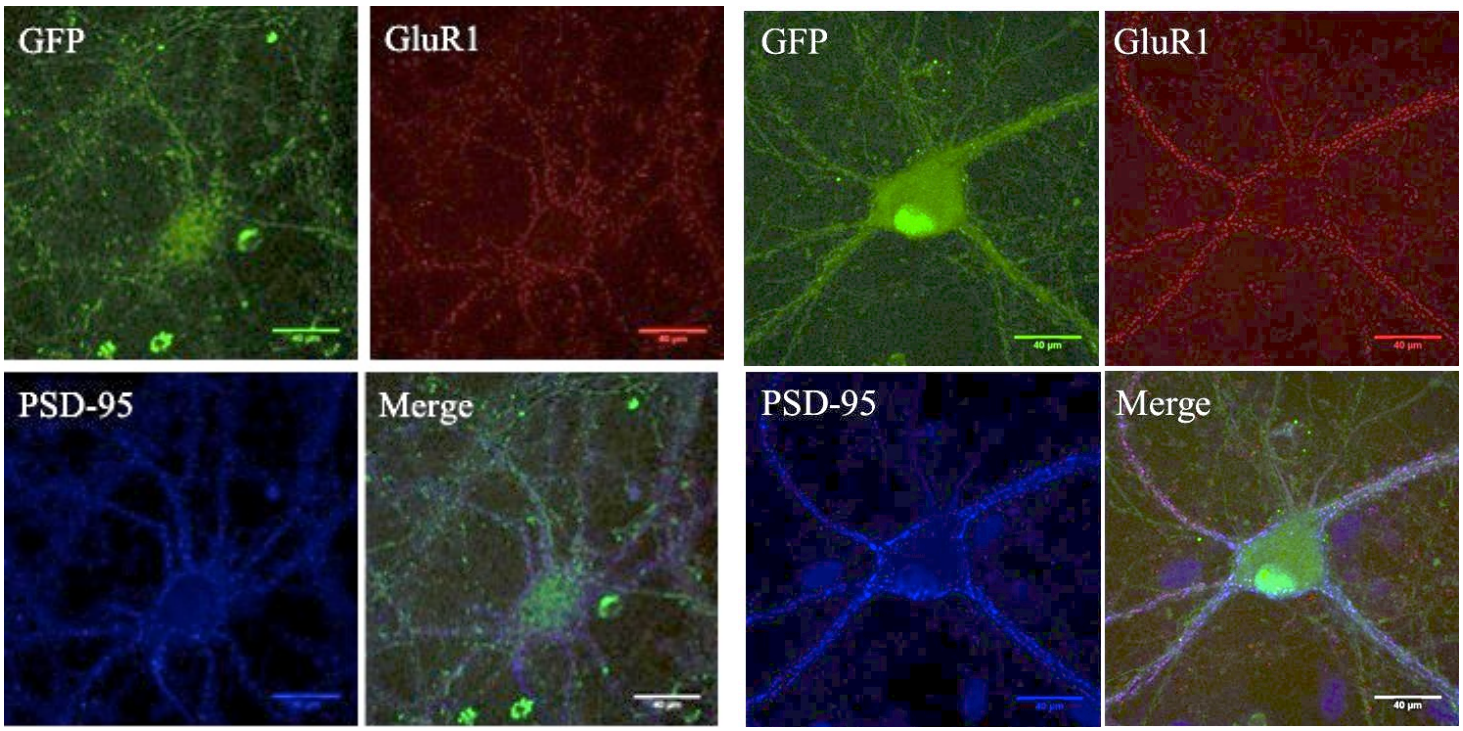

c)

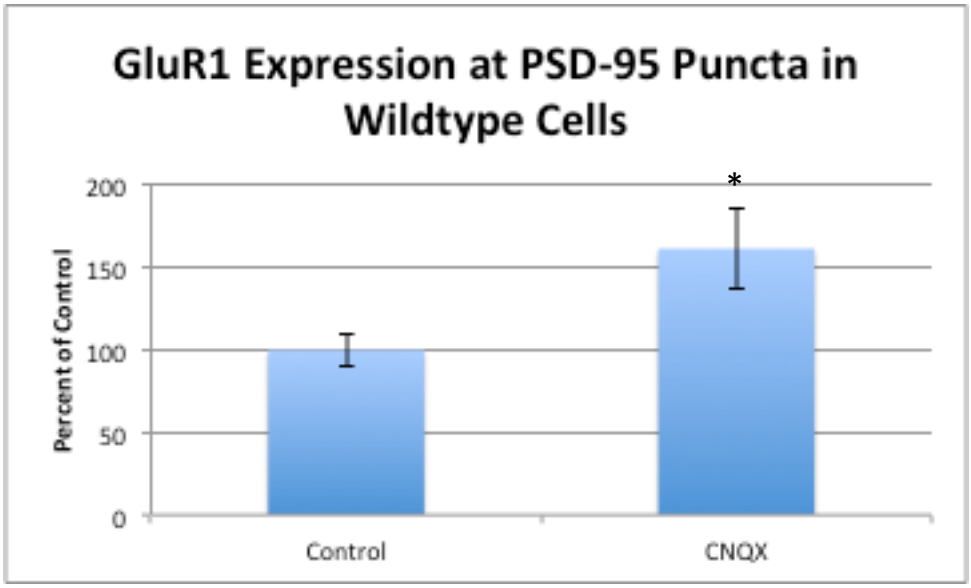

Figure 2. GluR1 Surface Staining in GFP Expressing Wildtype Mice.

(a) Control wildtype cells treated with media, expressing GFP, while stained for surface GluR1 and PSD-95. (b) Wildtype cells treated with CNQX, with the same staining. (c) Quantification of results show increased surface GluR1 expression in CNQX treated cells (one tailed t-test, p=0.01). All results normalized to the average wildtype control value.

a) Control

b) CNOX

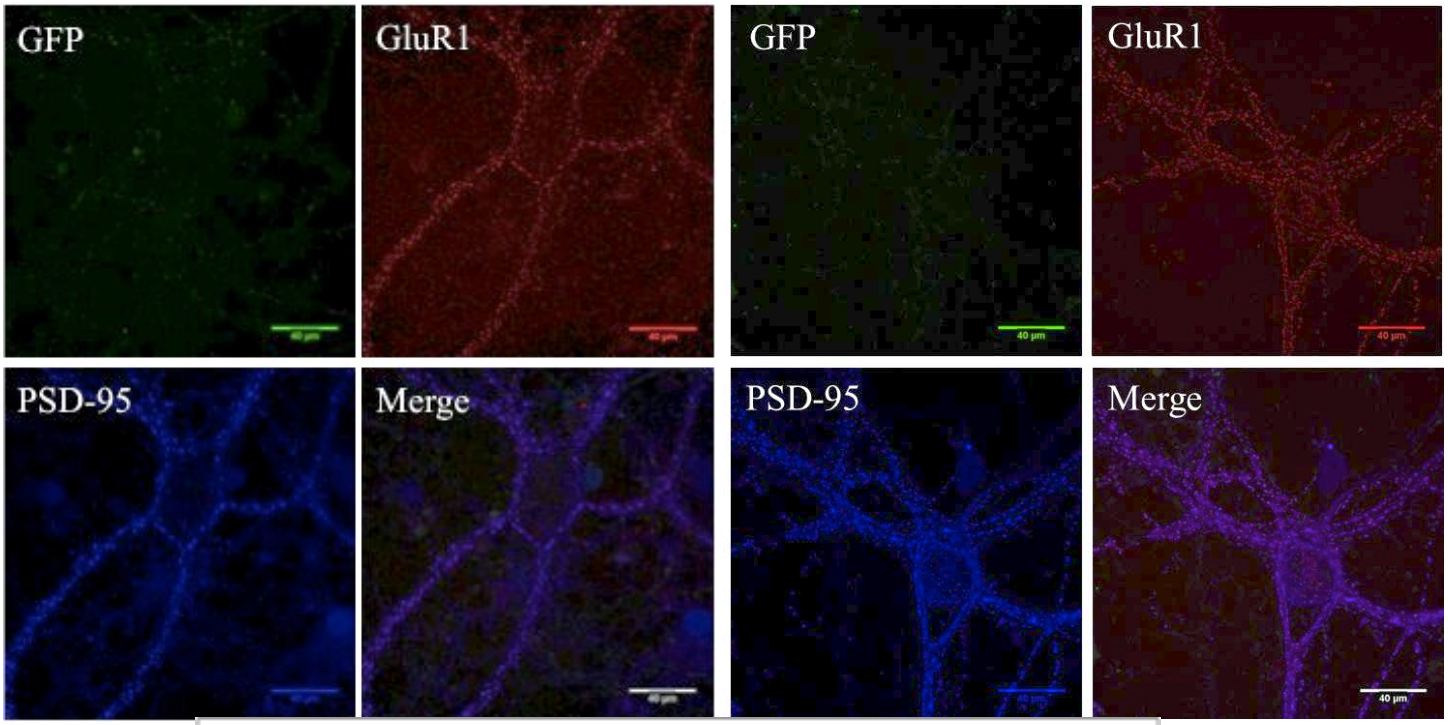

c)

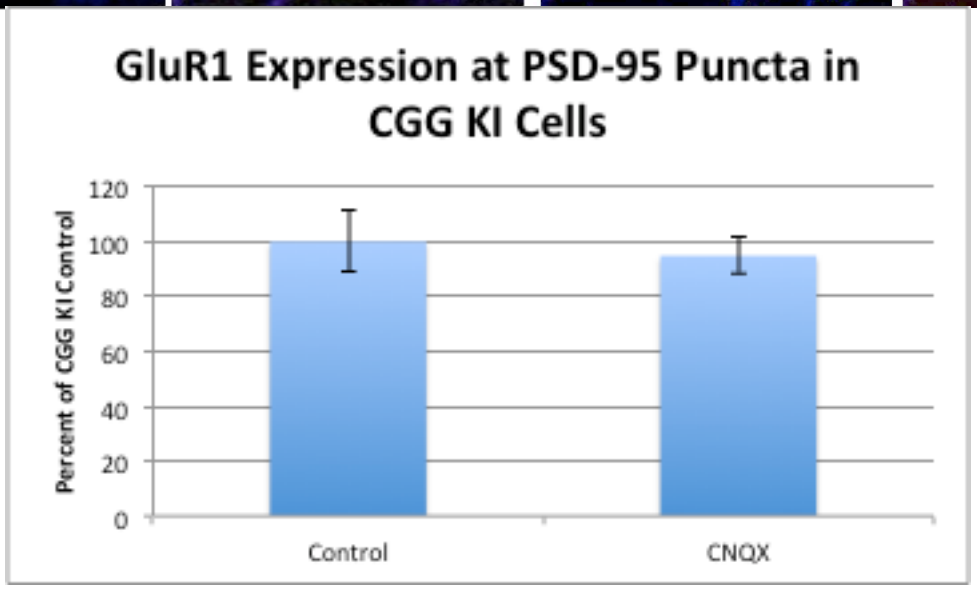

Figure 3. GluR1 Surface Staining in no GFP Expressing CGG KI Mice.

(a) CGG KI cells treated with media, not expressing GFP, while stained for surface GluR1 and PSD-95. (b) Cells treated with CNQX, same staining procedure. (c) Quantification of results show no difference in surface GluR1 expression between control and CNQX treated cells (p=0.35). Results normalized to the average CGG KI control value.

a)

b)

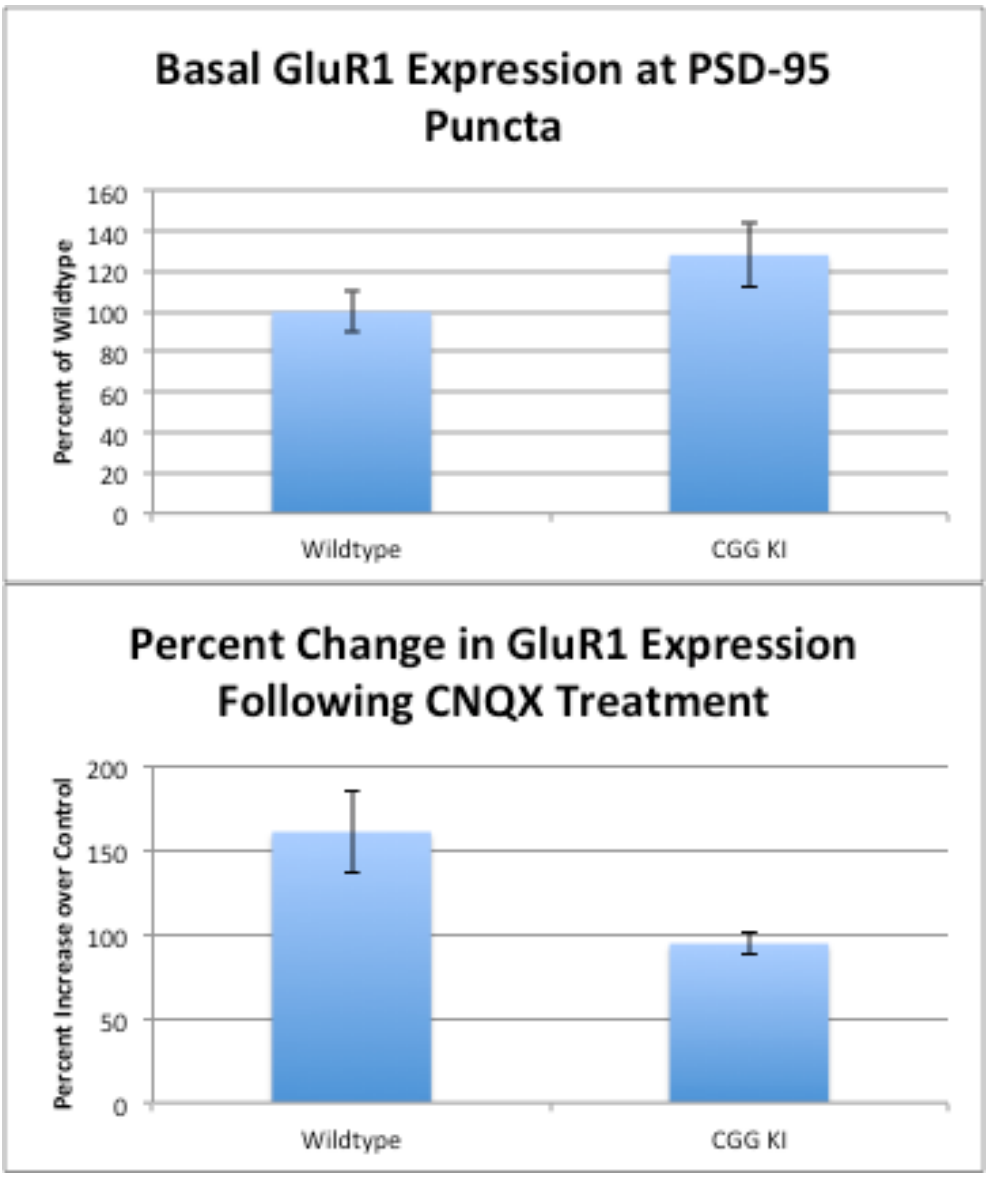

Figure 4. Quantification of GluR1 Surface Staining in Wildtype and CGG KI Mice.

(a) There was no significant difference in GluR1 expression between wildtype and CGG KI cells basally (p=0.06). Data normalized to the average wildtype control value. (b) Wildtype cells show a greater percent change in surface GluR1 expression following CNQX treatment. CGG KI cells remain at baseline.

a) Control b) CNQX

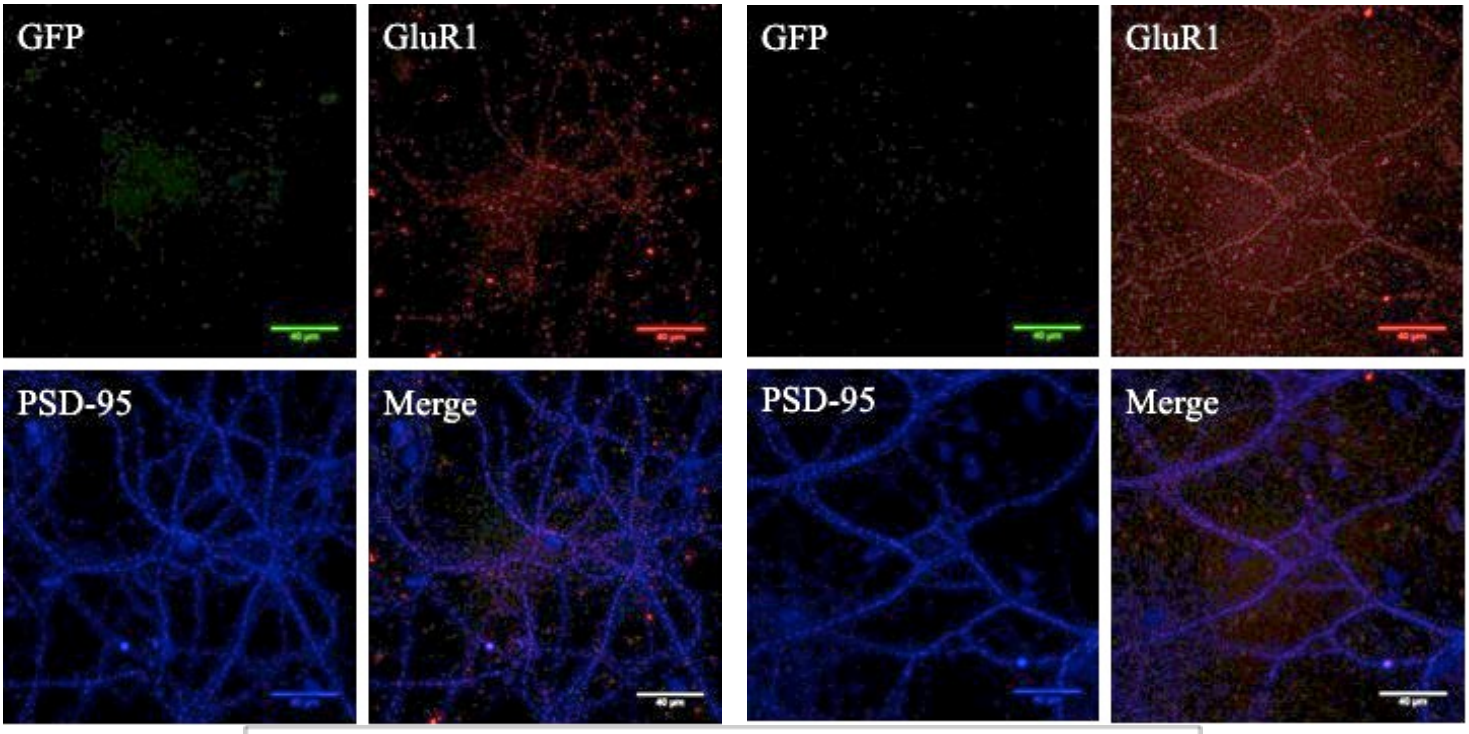

c)

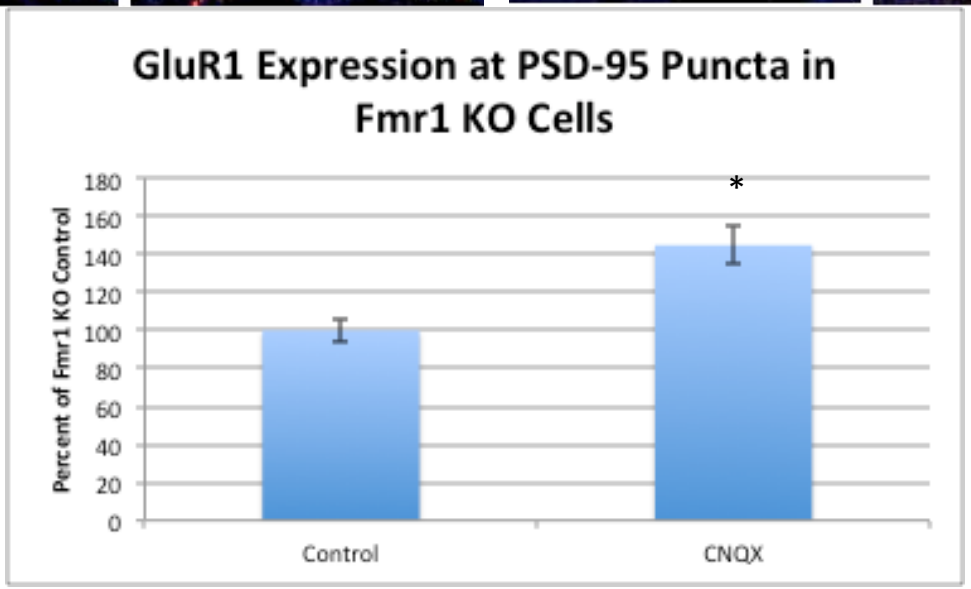

Figure 5. GluR1 Surface Staining in no GFP Expressing Fmr1 KO Mice.

(a) Fmr1 KO cells treated with media, not expressing GFP, while stained for surface GluR1 and PSD-95. (b) Cells treated with CNQX, same staining procedure. (c) Quantification of results show a significant increase in surface GluR1 expression after CNQX treated cells (p=0.0001). Results normalized to the average Fmr1 KO control value.

a)

b)

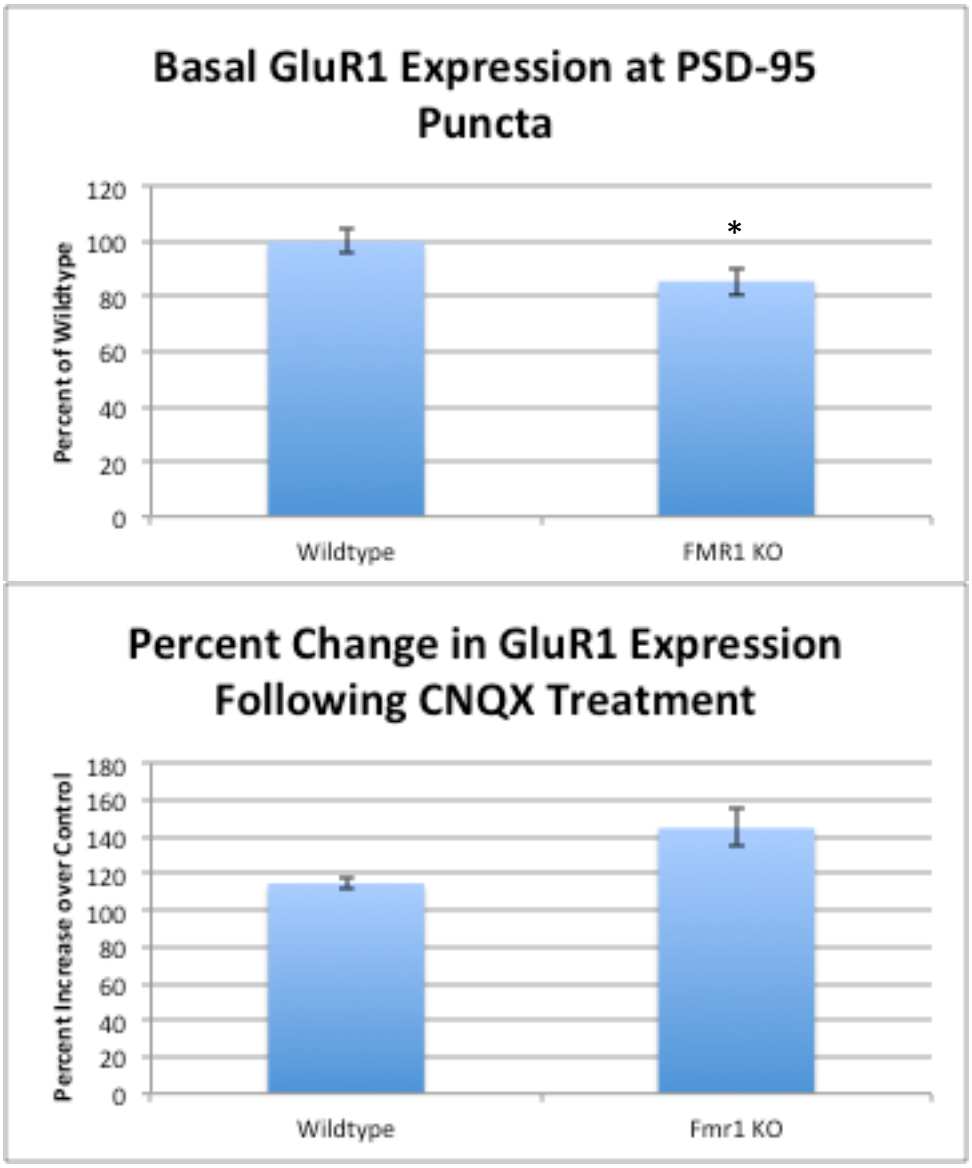

Figure 6. Quantification of GluR1 Surface Staining in Wildtype and Fmr1 KO.

(a) There is a significant decrease in surface GluR1 expression in Fmr1 KO cells compared to wildtype cells basally ($p=0.01$) Data normalized to wildtype control (b) Fmr1 KO cells show a greater percent change than wildtype cells in GluR1 expression following CNQX treatment.

a) Wildtype b) Fmr1 KO

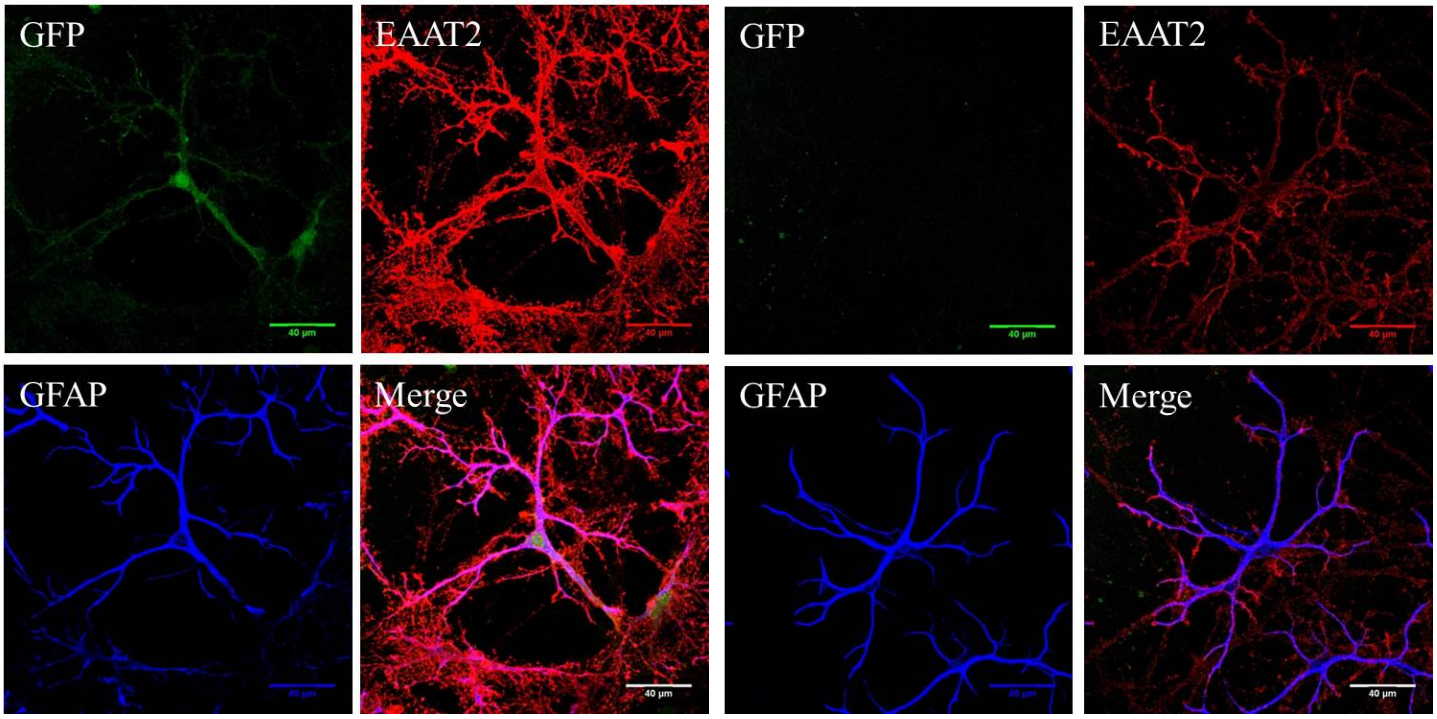

c)

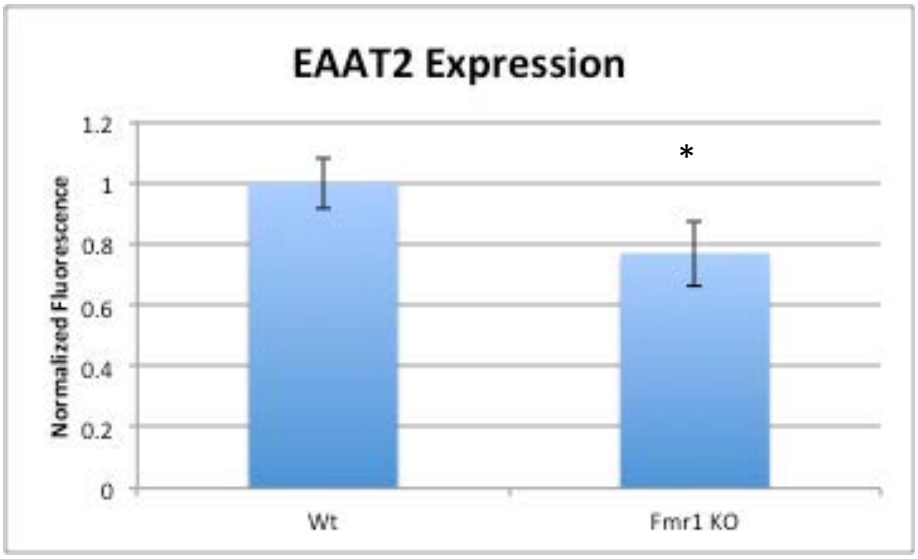

Figure 7. EAAT2 Staining in Wildtype and FMR1 KO Mice.

a) Wildtype glia expressing GFP, stained for EAAT2 and GFAP. (b) Fmr1 KO glia not expressing GFP, but same staining (c) Quantification of results. Statistically significant decreased EAAT2 expression in Fmr1 KO glia compared to wildtype control (p=0.04). All data normalized to the average wildtype control.

a) Wildtype

b) CGG KI

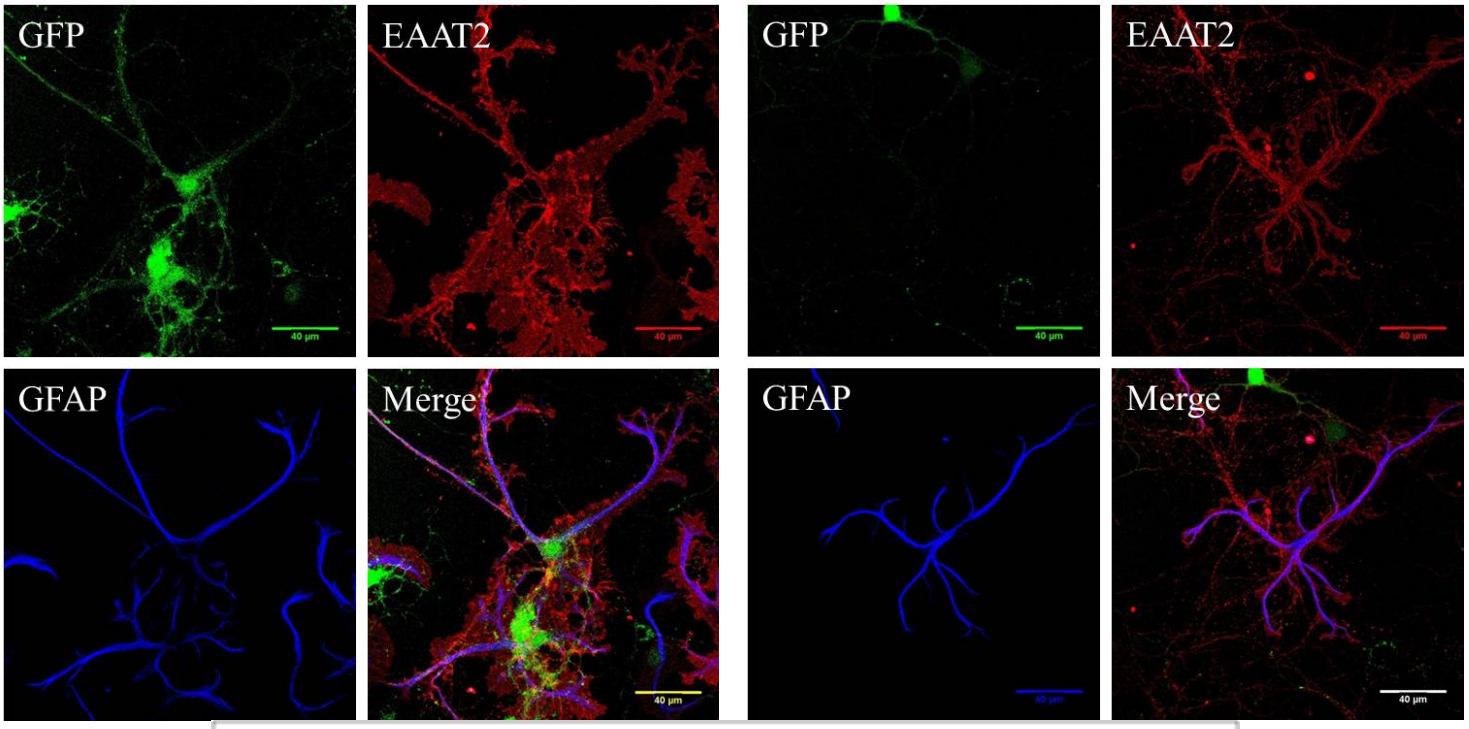

c)

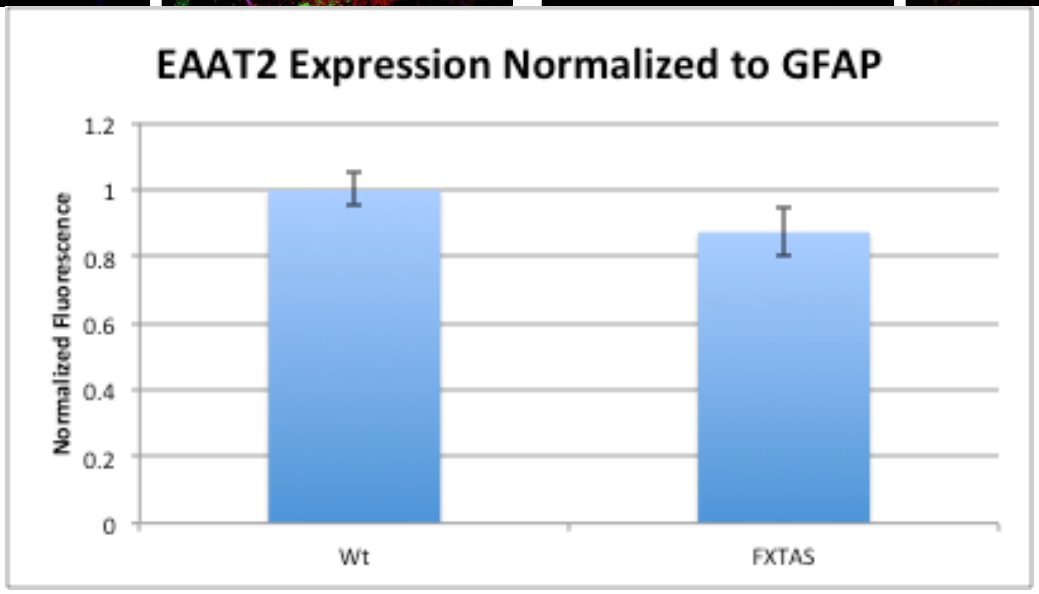

Figure 8. EAAT2 Staining in Wildtype and CGG KI Mice.

a) Wildtype glia expressing GFP, stained for EAAT2 and GFAP. (b) CGG KI glia not expressing GFP, but same staining (c) Quantification of results. There was no significant difference in EAAT2 expression in CGG KI glia compared to wildtype ($p=0.12$). When only EAAT2 expression was measured, there was also no significant difference ($p=0.36$, results not pictured). All data normalized to the average wildtype control.

a)

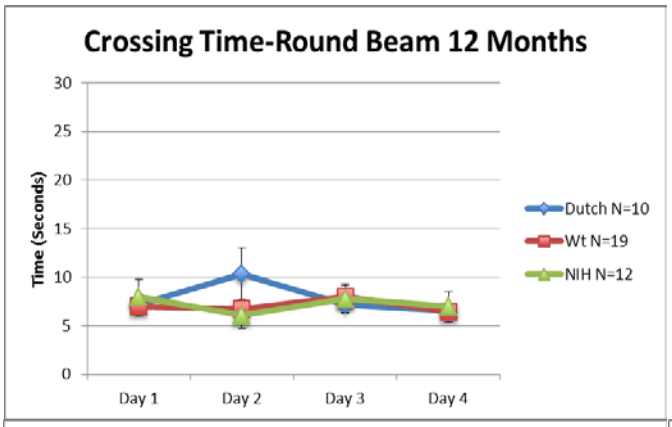

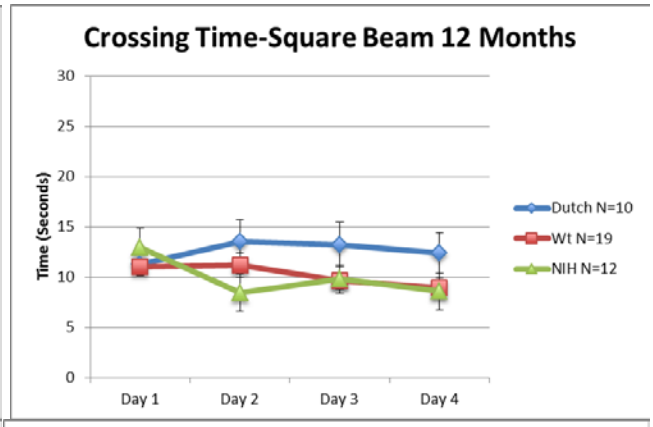

b)

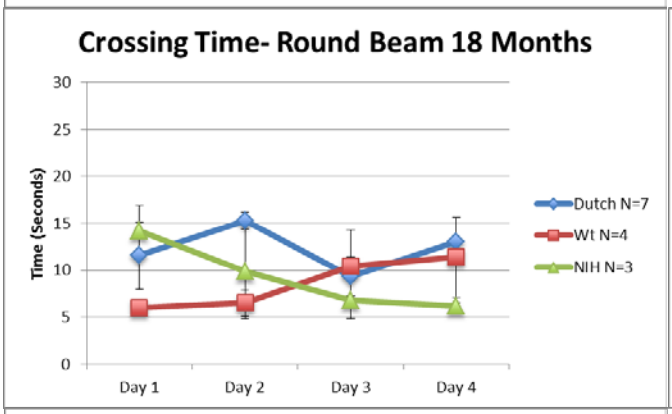

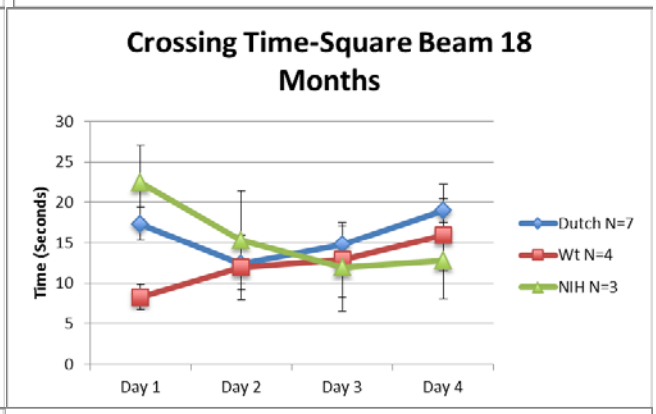

c)

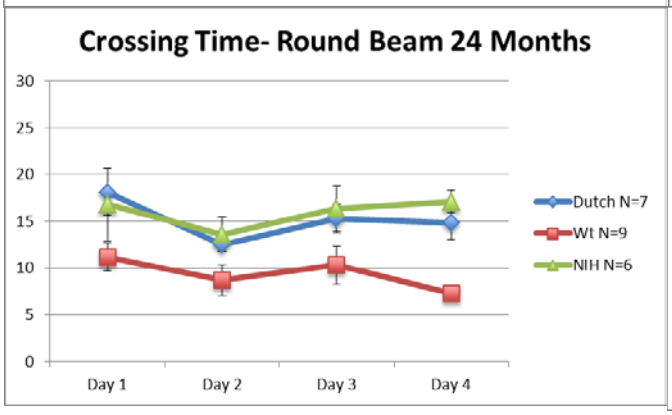

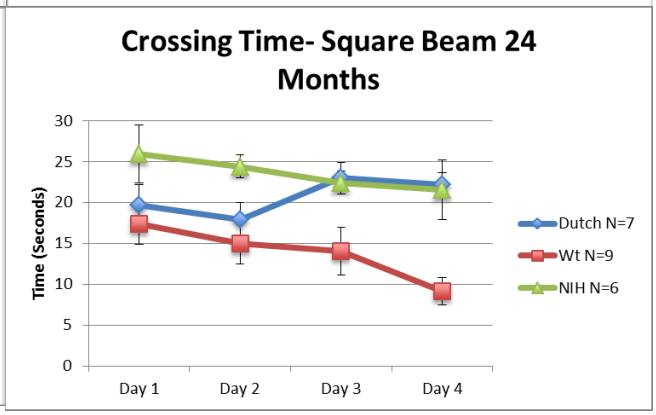

Figure 9. Crossing Time of the Dutch and NIH CGG KI mouse model with wildtype.

Crossing times are noted for each genotype on the round beam (left column) and round beam (right column). a) Mice tested at 12 months of age b) Mice tested at 24 months of age c) Mice tested at 24 months end stage.

Day 1	Round Beam p-value	Square Beam p-value
CGG KI vs Wt	*0.014	0.058
Dutch vs NIH	0.75	0.14
Dutch vs Wt	*0.018	0.5
NIH vs Wt	0.12	*0.047

Day 2	Round Beam p-value	Square Beam p-value
CGG KI vs Wt	*0.0079	*0.032
Dutch vs NIH	0.54	*0.049
Dutch vs Wt	0.062	0.39
NIH vs Wt	0.06	*0.027

Day 3	Round Beam p-value	Square Beam p-value
CGG KI vs Wt	*0.0094	*0.0016
Dutch vs NIH	0.69	0.8
Dutch vs Wt	0.064	*0.022
NIH vs Wt	0.06	*0.033

Day 4	Round Beam p-value	Square Beam p-value
CGG KI vs Wt	*3.2E-06	*1.1E-05
Dutch vs NIH	0.31	0.86
Dutch vs Wt	*0.0006	*2.2E-05
NIH vs Wt	*4.6E-06	*0.0023

Figure 10. Statistical Analysis of Crossing Times Between the Dutch and NIH CGG KI Mouse Model along the Wildtype at End Stage.

Statistical Analysis at the end stage shows a significant difference between the Dutch and NIH model at Day 2 on the square beam only. Both CGG KI models were significantly different from the wildtype on every day. Only on days 1-2 on the square beam, did the Dutch show a significant difference in crossing times. The “CGG KI” represents the NIH and Dutch results pooled together, then statistically tested against the wildtype. This demonstrates the effect of the CGG KI in general.

a)

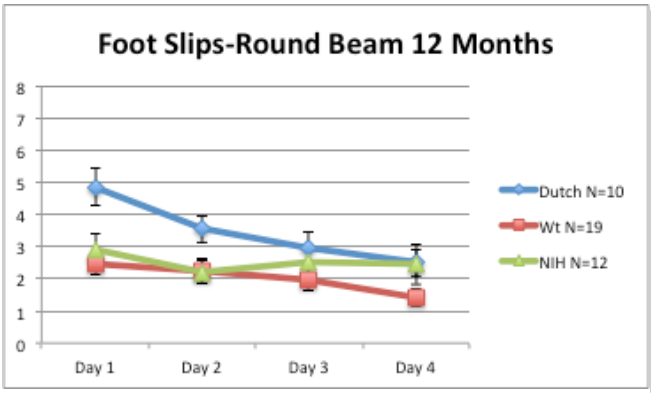

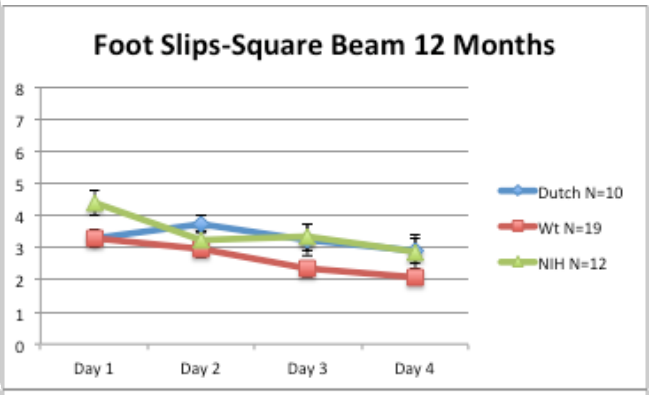

b)

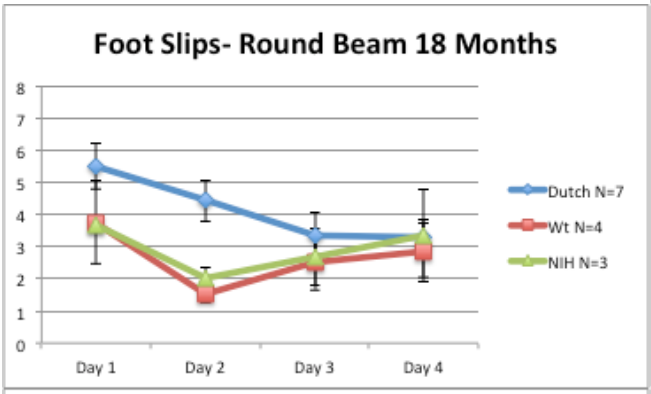

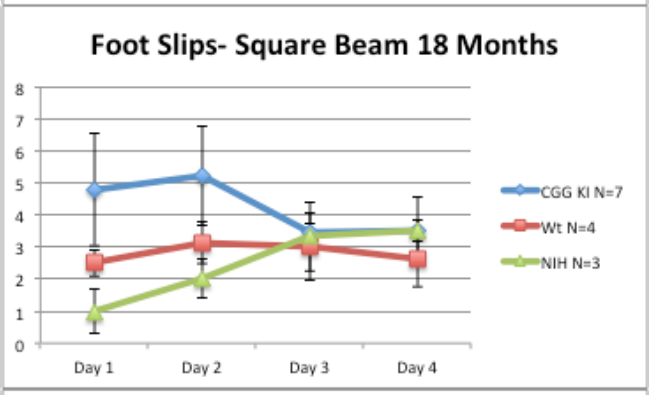

c)

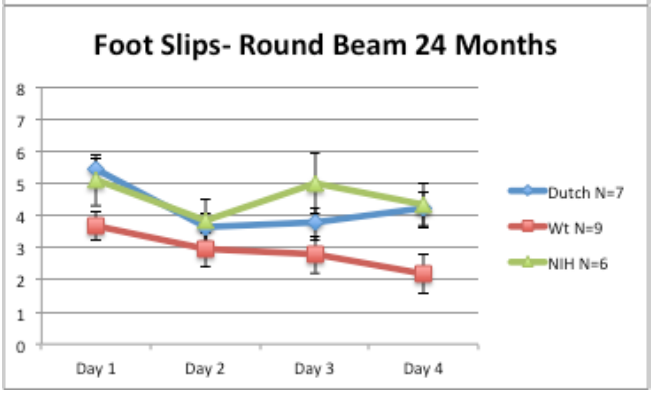

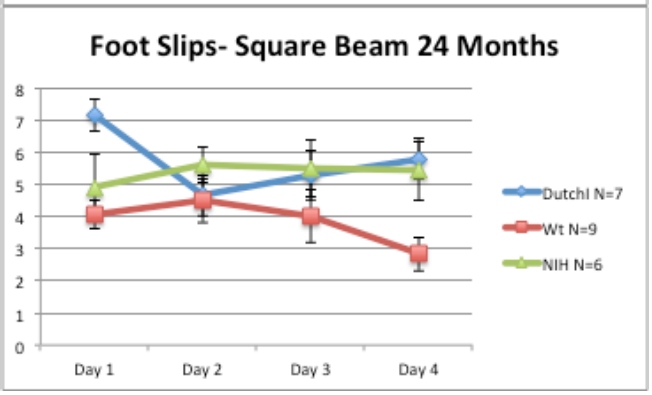

Figure 11. Foot Slips of the Dutch and NIH CGG KI mouse model with wildtype.

Foot slips are noted for each genotype on the round beam (left column) and round beam (right column). a) Mice tested at 12 months of age b) Mice tested at 24 months of age c) Mice tested at 24 months end stage.

a)

b)

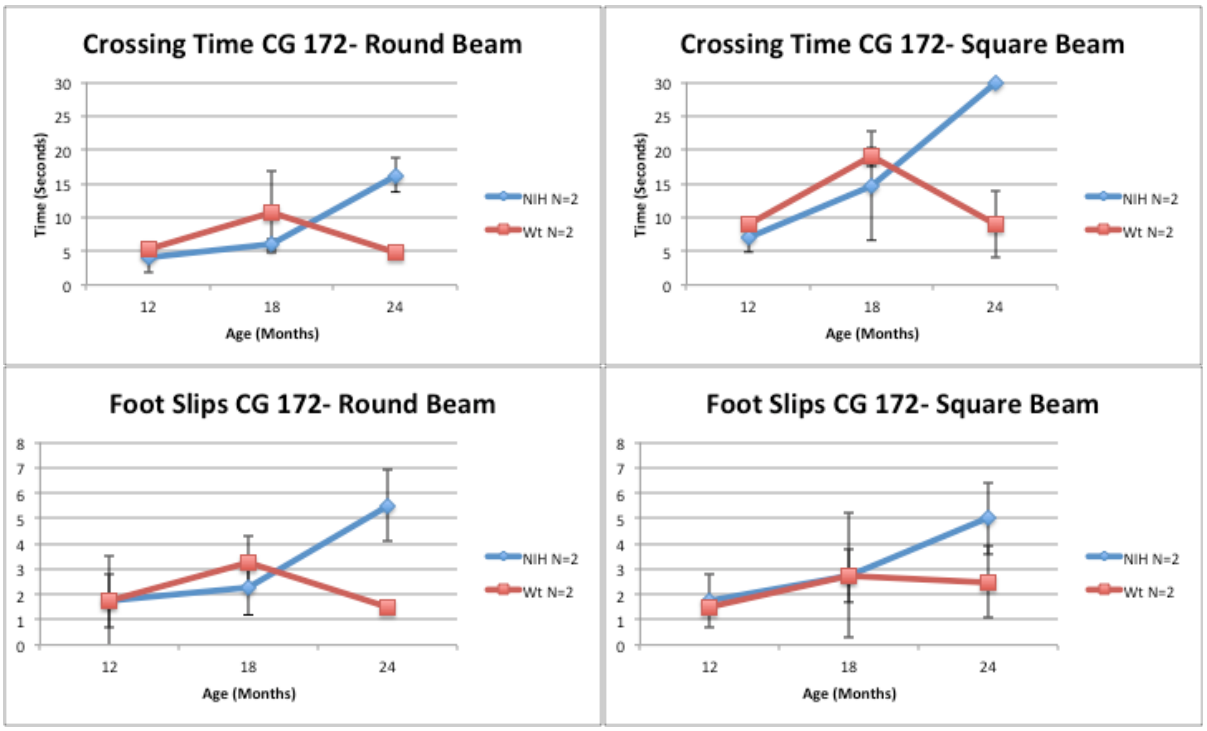

Figure 12. Crossing Times and Foot Slips of the NIH CGG KI Mouse Model Compared to Wildtype of a Single Cage.

a) Crossing time for a sample of the NIH and wildtype cage over time on the round beam (left column) and square beam (right column). b) Foot slips are noted for each genotype on the round beam (left column) and round beam (right column). Not enough data to perform a statistical analysis.

Discussion

Overall the CGG KI mice demonstrate a key pathological indicator of Fragile-X Tremor and Ataxia Syndrome illustrated by several studies: decreased FMRP expression compared to wildtype control cells (Bardoni et al 2002, Greco et al 2006, Todd et al 2013). Although in this experiment the CGG KI mice did not show a significant decrease in FMRP expression from the wildtype mice, it is difficult to draw any conclusions due to the small sample size used in this experiment. Furthermore it was difficult to quantify FMRP when other fragments of FMRP existed and the amount of tubulin expressed in lane was not consistent. On the other hand, the balance beam behavioral study was successful in illustrating key symptoms of FXTAS. Because defects in coordination were most evident during the 24-month of age testing period, the Dutch and NIH CGG KI mouse models proved to be accurate representations of FXTAS. Interestingly the average age of onset for FXTAS in humans is 60 years, at which the tremor often precedes the ataxia like symptoms by one to several years (Leehey et al 2007). Since there were little differences in the results of the 12 and 18-month testing periods within both genotypes, this further gives evidence to the finding that the mouse model shows symptoms mostly in the late stage (Entezam et al 2007). Although the wildtype and the NIH CGG KI models both show a decline in coordination over time, this decline is far more pronounced in the NIH CGG-KI models at the late stage. Thus both of these mice seem to replicate the late onset decline in motor coordination associated with FXTAS.

It has been noted that unlike the Dutch model, the NIH mouse model retains a larger region of the mouse 5'UTR surrounding the CGG repeat, which includes a TAA

stop codon (Entezam et al 2007, Todd et al 2013). Placing the NIH mouse sequence, but not the Dutch mouse sequence, just proximal to the repeat blocked translation in the +1 (Gly) frame, resulting in the novel polyglycine protein only in the Dutch mouse (Todd et al 2013). The balance beam experiments between the NIH and Dutch CGG-KI mouse models of FXTAS shed light on potential deviations of motor behavior this polyglicine product may cause. One would predict that the Dutch model would have greater deficits in motor coordination than the NIH model, due to the presence of this product, but this was not the case. There were no significant differences between either of the models at various days of a testing period that subsided during the course of the testing. However this finding does not rule out the possibility of different aspects of coordination being altered by the genotype. At the time in which the results were analyzed for this thesis, there were still mice that would have reached 18 or 24 months old within the next year. A longitudinal study of specific Dutch mice would illustrate differences as well. Thus an increased sample size could validate any of the findings thus far. All in all, these findings demonstrate that the Dutch and NIH CGG KI exhibit strong differences in motor coordination from wildtype mice, while maintaining little differences between each other. Due to shared late onset pathology with FXTAS, it is more likely that cellular and molecular observations noted in these models have a higher probability of bearing validity in the human condition.

The results of Figure 2 demonstrate that homeostatic plasticity can be induced in cell culture through the application of CNQX for six hours. CNQX treated cells displayed increased levels of GluR1 and mimicked the effect of long term TTX application in a way that was AMPA receptor specific, thus providing another method to experimentally

induce HSP (Soden et al 2010). Only the Wt GFP expressing cells in the GFP/KO cell cultures showed a significant increase in GluR1 expression, thus establishing a reliable control. Interestingly the control CGG KI neurons did not exhibit significantly increased levels of basal GluR1. Contrary to the wildtype cells, the CGG KI cells showed no significant change in GluR1 expression after CNQX application. This suggests that the CGG KI neurons were not able to regulate their own excitability and restore a preferred response to an environmental change, which in this case was the application of CNQX.

Given the crucial role of FMRP in maintaining HSP (Henry et al 2011; Soden et al 2010), perhaps the decreased FMRP expression in the CGG KI neurons might prevent them from regulating their own excitability properly. Furthermore the presence of toxic CGG-containing Fmr1 mRNA and the production of RAN translation products might be preventing the CNQX induced translation of AMPA receptors (Renoux et al 2012). Subsequently the abundance of GluR1 on the surface of the CGG KI cells might be one of the reasons that underlie the increased susceptibility to hyper excitability and altered inhibitory transmission in noted in other findings (D'hulst et al 2009). Taken together, the CGG KI cells demonstrate a defect in the pathway of homeostatic plasticity.

In contrast to the findings of the CGG KI neurons, the Fmr1 KO neurons responded to the CNQX treatment similarly as the wildtype neurons did. Although the Fmr1 KO cells expressed more surface GluR1 than the wildtype cells basally, these cells still demonstrated a significant increase in GluR1 expression following CNQX treatment, which differed considerably from the CGG KI cells. Perhaps the presence of the toxic CGG-containing Fmr1 mRNA renders greater pathology here than no Fmr1 mRNA all together. At first this finding seems to contradict with previous results showing impaired

GluR1 translation in Fmr1 KO mice following APV and TTX treatment (Soden et al 2010). However, the study by Soden and Chen accounted for only Retinoic Acid dependent dendritic translation. Perhaps RA-independent translation might be occurring to allow increased GluR1 expression following CNQX treatment through a different mechanism. Furthermore the study induced homeostatic plasticity through a different method by using an NMDA receptor antagonist and TTX, which together would block all NMDA channels in addition to all voltage gated sodium channels. It seems that there are many different experimental mechanisms to induce HSP, which in turn may correlate with the way neurons respond accordingly to various environmental stimuli.

In conjunction with previous findings showing that GLT1 levels are reduced in Fmr1 KO mice (Higashimori et al 2013), the Fmr1 KO hippocampal cell cultures demonstrated significantly reduced excitatory amino acid transporter 2 (EAAT2) levels compared to wildtype cells. The dramatically decreased levels of glutamate transporter would not allow astrocytes to clear glutamate from the synapse as efficiently. Subsequently this would naturally lead to higher levels glutamate in the synapse, ultimately resulting in increased activation of glutamatergic synapses, thus potentially activating various downstream pathological mechanisms. Subsequently these neurons might require stronger inhibitory post-synaptic potentials in order for their activity to be regulated. Perhaps many of the cognitive problems associated with FXS might originate from over excitability in these hippocampal neurons.

The CGG KI glia did not show a significant decrease in EAAT2 expression, unlike the Fmr1 KO glia. In fact both raw EAAT2 levels and EAAT2 levels normalized to GFAP in CGG KI glia did not yield a significant difference with wildtype glia. This

finding seems to disagree with previous research showing reduced excitatory amino acid transporter1 (EAAT1) levels in the cerebellum of post-mortem human premutation carriers with FXTAS (Pretto et al 2014). It is worthy to note that this study examined cultured hippocampal mice glia, while the previously mentioned study (Pretto et al 2014), examined human glia in brain slices. Thus these different results could highlight potential differences in human and mouse samples or even show differences in glutamate transport of brain regions. Furthermore fairly different staining techniques were used. Perhaps normalizing to another glial protein would give more conclusive results, as GFAP expression has been shown to be reduced in Fmr1 KO mice glia and not CGG KI (Yuskaitis et al 2010). Repeated experiments and a larger sample size are needed to make permanent conclusions. The possibility of impaired glutamate transport throughout the entire brain of FXTAS patients still remains.

When compared to the results in the Fmr1 KO glia, the magnitude of the decrease in EAAT2 expression in the CGG KI cells was not as substantial. Other studies have characterized the presence of EAAT2 promoters, which show elevated expression in astrocytes, along with other regulators of EAAT2 transcription (Su et al 2002). It may be that FMRP could play a crucial role in such transcriptional processes. Since the EAAT2 levels were higher in FXTAS than in FXS model cells, it appears that the levels of EAAT2 expression in glia seem to correlate with the amount of FMRP expression. In fact it has been shown that SLC1A2, the gene that codes for EAAT2, is indeed a target of FMRP (Darnell et al 2011). Since FMRP is a negative regulator of translation, it would seem that one would expect increased EAAT2 levels in Fmr1 KO cells. However it could

be that FMRP instead regulates the stability of SLC1A2 mRNA, resulting in decreased stability in the absence of FMRP.

Although there appeared to be no statistically significant decrease in EAAT2 expression in the CGG KI cells, the increased basal GluR1 levels and altered homeostatic plasticity might account for the main reason behind the state of neuronal hyperexcitability observed in FXTAS. Thus neuronal properties rather than glial properties might be leading to this phenotype in CGG KI cells, whereas glial properties might underlie hyperexcitability in Fmr1 KO cells. All in all these findings suggest fairly different mechanisms underlying seemingly similar pathologies in Fragile-X Syndrome and Fragile-X Tremor Ataxia Syndrome. Ultimately these differences should be taken into account, when treating patients with FXTAS or FXS.

Acknowledgements

Thank you to my sponsor and my principal investigator Dr. Peter Todd for giving me the opportunity to conduct research for the University of Michigan Department of Neurology. Neurology is a field that has interested me from the very beginning, and my time in the Todd lab has even furthered my interests. His scientific guidance was a key part in the development of this thesis and on myself as a student. No matter which specialty I wish to pursue in medical school, I will always carry with me the principals of proper investigation I have learned from Dr. Todd. I would also like to thank my co-sponsor Dr. Richard Hume for sponsoring me over the course of two years while I was conducting my research. Additionally I would like to thank Dr. Catherine Collins for agreeing to be a reader for my thesis. The principals I had learned from Dr. Collins and Dr. Hume in MCDB 351 and 455 helped me understand my work on a much deeper level. Furthermore I would like to thank Dr. Michael Sutton and his lab members at the University of Michigan Molecular and Behavioral Neuroscience Institute for allowing me to carry out the majority of my experiments in his lab.

Most importantly, I would like to personally thank Abigail Renoux for guiding me through every step of my experience in the Todd lab. She devoted a great deal of time teaching me every lab technique I know today, giving advice on my project, and proofreading my thesis. Without her help, none of this would have been possible. Lastly, thank you to everyone in the Todd and Sutton lab for providing technical help and being a great part of my college experience.

References

Aoto J, Nam CI, Poon MM, Ting P, Chen L. (2008) Synaptic signaling by all-trans retinoic acid in homeostatic synaptic plasticity. *Neuron, 60*, 308–20.

Bardoni, B., Mandel, J. L. Advances in understanding of fragile X pathogenesis and FMRP function, and in identification of X linked mental retardation genes. (2002), *Current opinion in genetics & development, 12*(3), 284-293.

Basuta, K., Narcisa, V., Chavez, A., Kumar, M., Gane, L., Hagerman, R., & Tassone, F. (2011). Clinical phenotypes of a juvenile sibling pair carrying the fragile X premutation. *American Journal of Medical Genetics Part A, 155*(3), 519-525.

Bear, Mark F., Kimberly M. Huber, and Stephen T. Warren. (2004). The MGluR Theory of Fragile X Mental Retardation. *Trends in Neurosciences 27*, 370-77. Web.

Bell, M. V., Hirst, M. C., Nakahori, Y., MacKinnon, R. N., Roche, A., Flint, T. J., Davies, K. E. Physical mapping across the fragile X: hypermethylation and clinical expression of the fragile X syndrome. (1991), *Cell, 64*(4), 861-866.

Berman, R. F., Buijsen, R. A., Usdin, K., Pintado, E., Kooy, F., Pretto, D., Hukema, R. K. Mouse models of the fragile X premutation and fragile X-associated tremor/ataxia syndrome. (2014), *Journal of neurodevelopmental disorders, 6*(1), 25.

Berman, R., F., Willemsen, R. Mouse models of fragile x-associated tremor ataxia. (2009), *J Investig Med., 57*, 837–841.

Bontekoe, C. J., Bakker, C. E., Nieuwenhuizen I., M., van Der Linde, H., Lans, H., de Lange, D., Hirst, M. C., Oostra, B. A. Instability of a (CGG)(98) repeat in the Fmr1 promoter. (2001), *Hum Mol Genet, 10*, 1693–1699.

Cao, Z., S. Hulsizer, F. Tassone, H.-T. Tang, R. J. Hagerman, M. A. Rogawski, P. J. Hagerman, and I. N. Pessah. (2012). Clustered Burst Firing in FMR1 Premutation Hippocampal Neurons: Amelioration with Allopregnanolone. *Human Molecular Genetics 21*, 2923-935. Web

Cao, Z., S. Hulsizer, Y. Cui, D. L. Pretto, K. H. Kim, P. J. Hagerman, F. Tassone, and I. N. Pessah. (2013). Enhanced Asynchronous Ca2 Oscillations Associated with Impaired Glutamate Transport in Cortical Astrocytes Expressing Fmr1 Gene Premutation Expansion." *J. Biol Chem. 288*, 13831-3841. Web.

Chen, Y., F. Tassone, R. F. Berman, P. J. Hagerman, R. J. Hagerman, R. Willemsen, and I. N. Pessah. (2009). Murine Hippocampal Neurons Expressing Fmr1 Gene

Premutations Show Early Developmental Deficits and Late Degeneration. *Hum Molec Gen. 19.*196-208. Web.

Clinical phenotypes of a juvenile sibling pair carrying the fragile X permutation. (2011), *Am. J. Med. Genet. A, 155A (3),* 519–525.

Cunningham, C.L., Martinez Cerdeno, V. Premutation CGG-repeat expansion of the Fmr1 gene impairs mouse neocortical development. (2010), *Hum. Mol. Genet., 20*, 64–79.

Danbolt, N. C. Glutamate Uptake. (2001), *Prog Neurobiol, 65(1),* 1–105.

Darnell, J. C., Van Driesche, S. J., Zhang, C., Hung, K. Y. S., Mele, A., Fraser, C. E., Darnell, R. B. (2011). FMRP stalls ribosomal translocation on mRNAs linked to synaptic function and autism. *Cell, 146(2),* 247-261.

D'hulst, Charlotte, Inge Heulens, Judith R. Brouwer, Rob Willemsen, Natalie De Geest, Simon P. Reeve, Peter P. De Deyn, Bassem A. Hassan, and R. Frank Kooy. "Expression of the GABAergic System in Animal Models for Fragile X Syndrome and Fragile X Associated Tremor/ataxia Syndrome (FXTAS)." (2009). *Brain Research, 1253*, 176-83. Web.

Dolen G, Osterweil E, Rao BS, Smith GB, Auerbach BD, Chattarji S, Bear MF. Correction of fragile-X syndrome in mice. (2007), Neuron. *56*, 955–962.

Entezam, A., Biacsi., R., Orrison, B., Saha, T., Hoffman, G. E, Grabczyk, E., Nussbaum, R., L., Usdin, K. Regional FMRP deficits and large repeat expansions into the full mutation range in a new fragile X premutation mouse model. (2007), *Gene, 395*, 125–134.

Feng, Y., Lakkis, L., Devys, D., Warren, S. T. Quantitative comparison of FMR1 gene expression in normal and premutation alleles. (1995), *American journal of human genetics*, *56*(1), 106.

Gainey, M. a, Hurvitz-Wolff, J. R., Lambo, M. E., & Turrigiano, G. G. Synaptic scaling requires the GluR2 subunit of the AMPA receptor. (2009). *The Journal of Neuroscience, 29(20),* 6479–89.

Greco, C. M. "Neuropathology of Fragile X-associated Tremor/ataxia Syndrome (FXTAS)." (2005) *Brain. 129*, 243-55. Web.

Hagerman, Randi Jenssen, and Paul J. Hagerman. Fragile X Syndrome: Diagnosis, Treatment, and Research. Baltimore: Johns Hopkins UP, 2002. Print.

Henry, F. E. A Fragile balance at synapses: New evidence supporting a role for FMRP in homeostatic plasticity. (2011). *The Journal of Neuroscience, 31*(18), 6617-6619.

Higashimori, H., L. Morel, J. Huth, L. Lindemann, C. Dulla, A. Taylor, M. Freeman, and Y. Yang. "Astroglial FMRP-dependent Translational Down-regulation of MGluR5 Underlies Glutamate Transporter GLT1 Dysregulation in the Fragile X Mouse." (2013) *Human Molecular Genetics, 22.10*, 2041-054. Web.

Hou, L. Antion, M., Hu, D., Spencer, C., M., Paylor, R., Klann, E. Dynamic Translational and Proteasomal Regulation of Fragile X Mental Retardation Protein Controls mGluR-Dependent Long-Term Depression. (2006), *Neuron , 51*, 441-454.

Huber, K. M., M. S. Kayser, and M. F. Bear. "Role for Rapid Dendritic Protein Synthesis in Hippocampal MGluR-Dependent Long-Term Depression." (2000), *Science 288*, 1254-256. Web.

Huber, K. M., S. M. Gallagher, S. T. Warren, and M. F. Bear. "Altered Synaptic Plasticity in a Mouse Model of Fragile X Mental Retardation." (2002), *Proceedings of the National Academy of Sciences 99.11*, 7746-750. Web.

Iliff A. J., Renoux A. J., Krans A., Usdin K., Sutton M. A., Todd, P. K. Impaired activity-dependent FMRP translation and enhanced mGluR-dependent LTD in fragile X premutation mice. (2013), *Hum. Mol. Genet., 22*, 1180–1192.

Jakawich, S. K., Nasser, H. B., Strong, M. J., McCartney, A. J., Perez, A. S., Rakesh, N., … Sutton, M. A. Local presynaptic activity gates homeostatic changes in presynaptic function driven by dendritic BDNF synthesis. (2010), *Neuron, 68(6)*, 1143–1158.

Jin, P.,Warren, S. T. Understanding the molecular basis of fragile X syndrome. (2000), *Human molecular genetics, 9*(6), 901-908.

Kaufmann, W. E., Cohen, S., Sun, H. T., Ho, G.. Molecular phenotype of Fragile X syndrome: FMRP, FXRPs, and protein targets. (2002), *Microscopy research and technique, 57*(3), 135-144.

Kim, D. Y., Kim, S. H., Choi, H. B., Min, C., Gwag, B. J. High abundance of GluR1 mRNA and reduced Q/R editing of GluR2 mRNA in individual NADPH-diaphorase neurons. (2001), *Mol. Cell. Neurosci. 17 (6)*, 1025–33.

Kleckner, N., W., Dingledine R. "Requirement for glycine in activation of NMDA-receptors expressed in Xenopus oocytes". (1988), *Science, 241 (4867)*, 835–7.

Laggerbauer, B., D. Ostareck, E. M. Keidel, and U. Fischer. "Evidence That Fragile X Mental Retardation Protein Is a Negative Regulator of Translation." (2001), *Human Molecular Genetics* 10.4: 329-38. Web.

Laube, B., Hirai, H., Sturgess, M., Betz, H., Kuhse, J. Molecular determinants of agonist discrimination by NMDA receptor subunits: analysis of the glutamate binding site on the NR2B subunit. (1997), *Neuron, 18 (3),* 493–503.

Leehey M. A. (2009). Fragile X-associated tremor/ataxia syndrome: clinical phenotype, diagnosis, and treatment. J. Invest. Med. 57, 830–836.

Ludwig, A. L., Espinal, G. M., Pretto, D. I., Jamal, A. L., Arque, G., Tassone, F., ... & Hagerman, P. J. (2014). CNS expression of murine fragile X protein (FMRP) as a function of CGG-repeat size. *Human molecular genetics, 23*(12), 3228-3238.

Ludwig, A.L., Hershey, J.W. Initiation of translation of the FMR1 mRNA occurs predominantly through 5'-end-dependent ribosomal scanning. (2011), *J. Mol. Biol., 407 (1),* pp. 21‑34

Marder, E., Prinz, A. Modeling stability in neuron and network function: the role of activity in homeostasis. (2002), *News and Reviews in Molecular, Cellular and Developmental Biology, 24*, 1145–54

Musumeci, Sebastiano A., Giuseppe Calabrese, Carmela M. Bonaccorso, Simona D'antoni, Judith R. Brouwer, Cathy E. Bakker, Maurizio Elia, Raffaele Ferri, David L. Nelson, Ben A. Oostra, and Maria Vincenza Catania. "Audiogenic Seizure Susceptibility Is Reduced in Fragile X Knockout Mice after Introduction of FMR1 Transgenes." (2007), *Experimental Neurology*, *203*, 233-40. Web.

Miller, K. D. Synaptic economics: competition and cooperation in synaptic plasticity. (1996), *Neuron, 17(3),* 371–374

Muddashetty RS, Kelic S, Gross C, Xu M, Bassell GJ. Dysregulated metabotropic glutamate receptor dependent translation of AMPA receptor and postsynaptic density-95 mRNAs at synapses in a mouse model of fragile X syndrome. (2007), *J. Neurosci, 27*, 5338–5348

Nalavadi, V. C., Muddashetty, R. S., Gross C., Bassell G.J. Dephosphorylation-induced ubiquitination and degradation of FMRP in dendrites: a role in immediate early mGluR-stimulated translation. (2012) *J. Neurosci*, *32*, 2582–2587.

Narayanan, U., Nalavadi, V., Nakamoto, M., Pallas, D. C., Ceman, S., Bassell, G. J., Warren, S. T. FMRP phosphorylation reveals an immediate-early signaling

pathway triggered by group I mGluR and mediated by PP2A. (2007), *The Journal of Neuroscience*, *27*(52), 14349-14357.

Nosyreva, E. D., Huber, K. M. Metabotropic receptor-dependent long-term depression persists in the absence of protein synthesis in the mouse model of fragile X syndrome. (2006), *J. Neurophysiol, 95*, 3291–3295.

Oberle, F. Rousseau, et al. Instability of a 550-base pair DNA segment and abnormal methylation in fragile X syndrome. (1991), *Science, 252*, 1097–1102.

Omrani, A., M. Melone, M. Bellesi, V. Safiulina, T. Aida, K. Tanaka, E. Cherubini, and F. Conti. "Up-regulation of GLT-1 Severely Impairs LTD at Mossy Fibre-CA3 Synapses." (2009), *The Journal of Physiology 587.19*, 4575-588. Web.

Poon MM, Chen L. Retinoic acid-gated sequence-specific translational control by RARalpha. (2008), *Proc Natl Acad Sci U S A.*, *105*, 20303–20308.

Pretto, D. I., Eid, J. S., Yrigollen, C. M., Tang, H. T., Loomis, E. W., Raske, C., Tassone, F. Differential increases of specific FMR1 mRNA isoforms in premutation carriers. (2015), *Journal of medical genetics*, *52*, 42-52.

Pretto, Dalyir I., Madhur Kumar, Zhengyu Cao, Christopher L. Cunningham, Blythe Durbin-Johnson, Lihong Qi, Robert Berman, Stephen C. Noctor, Randi J. Hagerman, Isaac N. Pessah, and Flora Tassone. Reduced EAAT1 and MGluR5 Expression in the Cerebellum of FMR1 Premutation Carriers with FXTAS. (2014), *Neurobiology of Aging*, *5*, 1189-197. Web.

Qin, M., Entezam, A., Usdin, K., Huang, T., Liu, Z. H., Hoffman, G. E., Smith, C. B. A mouse model of the fragile X premutation: effects on behavior, dendrite morphology, and regional rates of cerebral protein synthesis. (2011). *Neurobiol Dis., 42*, 85–98.

Qin, Mei, Ali Entezam, Karen Usdin, Tianjian Huang, Zhong-Hua Liu, Gloria E. Hoffman, and Carolyn B. Smith. A Mouse Model of the Fragile X Premutation: Effects on Behavior, Dendrite Morphology, and Regional Rates of Cerebral Protein Synthesis. (2011), *Neurobiology of Disease, 42*, 85-98. Web.

Renoux, A. J., & Todd, P. K. Neurodegeneration the RNA way. (2012), *Progress in neurobiology*, *97(2)*, 173-189.

Ronesi, J.A., Huber, K.M. Metabotropic glutamate receptors and fragile x mental retardation protein: partners in translational regulation at the synapse. (2008), *Sci. Signal., (5)*, 6

Rose, E. M., J. C. P. Koo, J. E. Antflick, S. M. Ahmed, S. Angers, and D. R. Hampson. "Glutamate Transporter Coupling to Na,K-ATPase." (2009), *Journal of Neuroscience, 29,* 8143-155. Web.

Singh, K., Pankaj G., S. Prasad. Fragile X Mental Retardation (Fmr-1) Gene Expression Is down Regulated in Brain of Mice during Aging. (2007), *Molecular Biology Reports, 34,* 173-181. Web.

Soden, M. E., and L. Chen. "Fragile X Protein FMRP Is Required for Homeostatic Plasticity and Regulation of Synaptic Strength by Retinoic Acid." (2010), *Journal of Neuroscience, 30,* 16910-6921. Web.

Su, Z. Z., Leszczyniecka, M., Kang, D. C., Sarkar, D., Chao, W., Volsky, D. J., Fisher, P. B. Insights into glutamate transport regulation in human astrocytes: cloning of the promoter for excitatory amino acid transporter 2 (EAAT2). (2003), *Proceedings of the National Academy of Sciences*, *100*(4), 1955-1960.

Sutton, M. A., Ito, H. T., Cressy, P., Kempf, C., Woo, J. C., Schuman, E. M. Miniature neurotransmission stabilizes synaptic function via tonic suppression of local dendritic protein synthesis. (2006), *Cell, 125(4),* 785–799.

Tassone F, Hagerman RJ, et al. Elevated levels of FMR1 mRNA in carrier males: a new mechanism of involvement in the fragile-X syndrome. (2000) *Am J Hum Genet., 66(1),* 6–15.

Tervonen, T.A., Louhivuori, V. Aberrant differentiation of glutamatergic cells in neocortex of mouse model for fragile X syndrome. (2009) *Neurobiol. Dis., 33 (2),* 250–259.

Thiagarajan, T. C., Lindskog, M., & Tsien, R. W. Adaptation to synaptic inactivity in hippocampal neurons. (2005), *Neuron, 47*(5), 725-737.

Todd, P.K., Mack, K.J. The fragile X mental retardation protein is required for type-I metabotropic glutamate receptor-dependent translation of PSD-95. (2003), *Proc. Natl. Acad. Sci. U. S. A., 100 (24),* 14374–14378

Todd, P. K., Oh, S. Y., Krans, A., He, F., Sellier, C., Frazer, M., Renoux, A. J., Chen, K. C., Scaglione, K. M., Basrur, V., Elenitoba-Johnson, K., Vonsattel, J. P., Louis E. D., Sutton, M. A., Taylor, J. P., Mills, R. E., Charlet-Berguerand, N., Paulson, H. L. CGG repeat-associated translation mediates neurodegeneration in fragile X tremor ataxia syndrome. (2013), *Neuron, 78,* 440–455.

Transcription of the FMR1 gene in individuals with fragile X syndrome. (2000) *Am. J. Med. Genet., 97,* 195–203.

Translational suppression by trinucleotide repeat expansion at FMR1. (1995), *Science, 268*, 731–734.

Turrigiano, G., Abbott, L. F., & Marder, E. Activity-dependent changes in the intrinsic properties of cultured neurons. (1994), *Science, 264*, 974–977.

Turrigiano, G. G., & Nelson, S. B. Hebb and homeostasis in neuronal plasticity. (2000), *Curr Opin Neurobiol, 10(3)*, 358–364.

Turrigiano, Gina G. "The Self-Tuning Neuron: Synaptic Scaling of Excitatory Synapses." (2008), *Cell, 135*, 422-35. Web.

Verkerk, A. J., Pieretti, M., Sutcliffe, J. S., Fu, Y. H., Kuhl, D. P., Pizzuti, A.,Warren, S. T. Identification of a gene (FMR-1) containing a CGG repeat coincident with a breakpoint cluster region exhibiting length variation in fragile X syndrome. (1991), *Cell, 65*(5), 905-914.

Weiler, I. J. Fragile X Mental Retardation Protein Is Translated near Synapses in Response to Neurotransmitter Activation. (1997), *Proceedings of the National Academy of Sciences, 94*, 5395-400. Web.

Westergaard, N., Sonnewald, U., & Schousboe, A.. Metabolic trafficking between neurons and astrocytes: the glutamate/glutamine cycle revisited. (1995), *Developmental neuroscience*, *17*(4), 203-211.

Willemsen, R., Hoogeveen-Westerveld, M., Reis, S., Holstege, J., Severijnen, L. A., Nieuwenhuizen, I. M., Schrier, M., van Unen, L., Tassone, F., Hoogeveen, A. T., Hagerman, P. J., Mientjes, E., J., Oostra, B., A. The FMR1 CGG repeat mouse displays ubiquitin-positive intranuclear neuronal inclusions; implications for the cerebellar tremor/ataxia syndrome. (2003), *Hum Mol Genet., 12*, 949–959.

Yuskaitis, C. J., Beurel, E., Jope, R. S. Evidence of reactive astrocytes but not peripheral immune system activation in a mouse model of Fragile X syndrome. (2010), *Biochimica et Biophysica Acta (BBA)-Molecular Basis of Disease*, *1802*(11), 1006-1012.

Zalfa, F., Eleuteri, B., Dickson, K. S., Mercaldo, V., De Rubeis, S., Di Penta, A., Bagni, C. A new function for the fragile X mental retardation protein in regulation of PSD-95 mRNA stability. (2007), *Nature neuroscience*, *10*(5), 578-587.

Zou, J. Y, Crews F. T. TNF alpha potentiates glutamate neurotoxicity by inhibiting glutamate uptake in organotypic brain slice cultures: neuroprotection by NF kappa B inhibition. (2006), *Brain Res. 1034 (1-2*): 11–24.